

Local norm-conserving pseudo-Hamiltonians

Andrea Bosin and Vincenzo Fiorentini

Dipartimento di Scienze Fisiche, Università di Cagliari, Via Ospedale 72, I-09124 Cagliari, Italy

Andrea Lastri

Dipartimento di Fisica, Università di Trento, I-38050 Povo, Italy

Giovanni B. Bachelet

Dipartimento di Fisica, Università di Roma "La Sapienza," Piazzale Aldo Moro 2, I-00185 Roma, Italy

(Received 17 February 1994)

A method is presented for the generation of valence-only local Hamiltonians, or pseudo-Hamiltonians, within the framework of the local-density-functional theory. Extensive transferability tests for atoms and crystals show that the performance of pseudo-Hamiltonians in density-functional-theory calculations matches the standards of other state-of-the-art methods. These pseudo-Hamiltonians represent a useful tool for quantum Monte Carlo simulations of many *sp*-bonded valence-only systems.

PACS number(s): 31.15.-p, 31.15.Ew, 71.10.+x

I. INTRODUCTION

When dealing with Green's function Monte Carlo (GFMC) techniques [1], the strong Z dependence of the simulation time needed to achieve low enough statistical errors in the computation of the relevant physical quantities for an atomic system [2] puts a very low upper bound on the number of electrons that can be accounted for simultaneously in quantum simulations of real atomic, molecular, and solid-state systems [3–5]. Together with the consideration that many properties of interest do not directly depend on the atomic cores (which are almost identical in atoms, molecules, and solids), we arrive in a natural way at the idea of a valence-only Hamiltonian replacing the full-core one in the description of the valence properties of the system. This idea, although not new [6], represents a lively branch of solid-state physics [7], where important results based on different methods of investigation and new theoretical developments [8] continue to blossom. Unfortunately the state-of-the-art valence-only Hamiltonians, which all stem from the nonlocal norm-conserving pseudopotential introduced by Hamann, Schlüter, and Chiang in 1979 [9], are not suitable for GFMC techniques (Sec. II A) without additional approximations [5]. The need for a valence-only operator specific to GFMC methods has led Bachelet, Ceperley, and Chiochetti [10] to the development of a local pseudo-Hamiltonian (Sec. II). Up to now, however, only very few atomic pseudo-Hamiltonians have been available. In addition Foulkes and Schlüter [11] have pointed out that only those elements for which the single-electron valence eigenvalues follow the "natural" order, $\epsilon_s \leq \epsilon_p \leq \epsilon_d \leq \dots$, can be described by a *local* pseudo-Hamiltonian (which rules out transition metals [12]). In spite of these limitations such an operator has been the first and for a long time the only choice for solid-state GFMC studies. For example, it was successfully used by

Li, Ceperley, and Martin [13] in the first GFMC simulation of an extended system (the Si crystal), a calculation well beyond the possibilities of the last-generation computers without the use of a pseudo-Hamiltonian. Since pseudo-Hamiltonians are, to date, the most practical way to perform GFMC quantum simulations for systems containing atoms heavier than neon, it seemed to us a good idea to obtain accurate pseudo-Hamiltonians for more and more elements in those regions of the periodic table where the method works well, leaving to alternative methods, which are more elaborate and introduce additional approximations, the task of tackling those elements for which pseudo-Hamiltonians are either impossible or more difficult to obtain [5]. For the construction of pseudo-Hamiltonians (as well as nonlocal pseudopotentials) we stick to the density functional theory–local density approximation (DFT-LDA) framework [14] and to the main ideas of Ref. [9], suitably extended for our aim (Secs. II C and III). We have generated several pseudo-Hamiltonians for the second and third rows of groups IIIB, IVB, VB, VIB, and VIIB as well as alkali metals like Li and Na and a first-row element like C (Sec. IV B). If accurate natural orbitals [15] become available for more and more elements, then the method presented here will have a straightforward extension to exact many-body atoms. For the atoms considered in this work, however, DFT-LDA ions should provide an excellent approximation [16]. We have tested the transferability of the generated operators in different ways (always within the DFT-LDA) using more severe transferability checks than is usually done with norm-conserving pseudopotentials (Sec. IV C). The results (Sec. IV) are extremely good in most cases; for our representative first-row atom, carbon, they are not of the same quality. Our results also confirm the common finding, recently emphasized by Teter [17], that the usual logarithmic derivative tests are not always conclusive from the point of view of transferabil-

ity, and other tests involving the self-consistent response of the system are more appropriate (Sec. IV C). As far as *portability* is concerned (i.e., to what degree of accuracy pseudo-Hamiltonians can be trusted as physically accurate effective ions outside the DFT-LDA framework [16]), we rely on the very encouraging results of Ref. [10] on atoms and molecules and of Ref. [13] on the bulk Si crystal, and leave further portability tests to future work. At the end of this Introduction it may be worthwhile pointing out that, besides their interest for GFMC quantum simulations, pseudo-Hamiltonians can suitably replace nonlocal pseudopotentials in connection with many other methods of investigation [11] since their manipulations are in general easier than those of nonlocal pseudopotentials: for example, they were recently used for the study of alkali-metal clusters [18].

Atomic units are used throughout the paper unless otherwise specified.

II. THEORY

A. The pseudo-Hamiltonian

The reason why a straightforward use of nonlocal pseudopotentials together with GFMC methods is not possible is connected with the need of positive Green's functions and with the so-called fixed-node approximation [19]. We are not going to describe in detail GFMC and its fixed-node approximation but we need to recall some aspects which are essential for the development of the pseudo-Hamiltonian [10,20]. In fixed-node GFMC we are faced with the following boundary condition problem (we use the notation \hat{H}^{PS} for the electronic Hamiltonian since we always deal with pseudo, valence-only operators):

$$\begin{aligned} \hat{H}^{PS}\Psi(\mathbf{R}) &= E^{FN}\Psi(\mathbf{R}) \quad \forall \mathbf{R} \in D, \\ \Psi(\mathbf{R}) &= 0 \quad \forall \mathbf{R} \in \partial D, \end{aligned} \quad (1)$$

and we look for the lowest energy eigenstate $\Psi(\mathbf{R})$ that never changes sign in the region D of the many-electron configuration space and vanishes on its frontier ∂D . This problem is well defined if the matrix elements $\langle \mathbf{R} | \hat{H}^{PS} | \mathbf{R}' \rangle$ vanish for $\mathbf{R} \neq \mathbf{R}'$ or, in other words, if \hat{H}^{PS} is a local operator; else from

$$\int \langle \mathbf{R} | \hat{H}^{PS} | \mathbf{R}' \rangle \Psi(\mathbf{R}') d\mathbf{R}' = E^{FN}\Psi(\mathbf{R}) \quad (2)$$

it follows that we might need to specify $\Psi(\mathbf{R})$ outside the

region D to know its action on $\Psi(\mathbf{R})$ inside it. The energy corresponding to the ground state of the boundary value problem E_0^{FN} is an upper bound to the true, unconstrained fermionic ground state E_0 of the Hamiltonian \hat{H}^{PS} in the whole configuration space; as ∂D approaches the exact nodal surface of the fermionic ground state, $E_0^{FN} - E_0$ vanishes quadratically [19]; this means that for a local operator \hat{H}^{PS} the fixed-node approximation has the very important feature of being variational and, since ∂D is defined by the nodes of an approximate trial function $\Psi_T(\mathbf{R})$ such that $\Psi_T(\mathbf{R}) > 0 \quad \forall \mathbf{R} \in D - \partial D$, $\Psi_T(\mathbf{R}) = 0 \quad \forall \mathbf{R} \in \partial D$, only the nodes of $\Psi_T(\mathbf{R})$ are important for E_0^{FN} , not its value anywhere else. Another fundamental reason to have a local Hamiltonian \hat{H}^{PS} comes from a basic hypothesis of GFMC: the Green's function

$$G(\mathbf{R}, \mathbf{R}', \tau) = \Psi_T(\mathbf{R}) \Psi_T^{-1}(\mathbf{R}') \langle \mathbf{R} | \exp(-\tau \hat{H}^{PS}) | \mathbf{R}' \rangle \quad (3)$$

has to be interpreted as a conditional probability density for each choice of Ψ_T , if we want to make use of the statistical result that the error decreases inversely proportionally to the square root of the number of steps. This means that $G(\mathbf{R}, \mathbf{R}', \tau)$ must be non-negative $\forall \mathbf{R}, \mathbf{R}' \in D$, and for all $\tau > 0$: this is automatic for "regular" Hamiltonians formed by a standard kinetic operator plus a local potential, but, unfortunately, not so for nonlocal pseudopotentials; even for more general local operators the Green's function may not satisfy this positivity requirement. Under which conditions does a local operator have a positive Green's function? To answer this question we recall an argument given previously [20]: we may first expand the generic local Hamiltonian \hat{H}^{PS} in powers of the momentum operator conjugate to \mathbf{R} , $\hat{\mathbf{P}} = -i\nabla_{\mathbf{R}}$,

$$\begin{aligned} \hat{H}^{PS} &= W(\mathbf{R}) + \sum_{\alpha=1}^{3N} K_{\alpha}(\mathbf{R}) \hat{P}_{\alpha} \\ &+ \sum_{\alpha,\beta=1}^{3N} T_{\alpha\beta}(\mathbf{R}) \hat{P}_{\alpha} \hat{P}_{\beta} + \dots, \end{aligned} \quad (4)$$

and then consider the tensor

$$c_{\alpha\beta}(\mathbf{R}_0, \tau) = \int (R - R_0)_{\alpha} (R - R_0)_{\beta} G(\mathbf{R}, \mathbf{R}_0, \tau) d\mathbf{R}. \quad (5)$$

If G is to be non-negative $\forall \mathbf{R}, \mathbf{R}' \in D$, and for all $\tau > 0$, then $c_{\alpha\beta}$ must be positive definite for each $\tau > 0$. For $\tau = 0$ we have

$$G(\mathbf{R}, \mathbf{R}_0, \tau = 0) = \Psi_T(\mathbf{R}) \Psi_T^{-1}(\mathbf{R}_0) \delta(\mathbf{R} - \mathbf{R}_0), \quad (6)$$

$$c_{\alpha\beta}(\mathbf{R}_0, \tau = 0) = 0. \quad (7)$$

Let us calculate the time derivative of $c_{\alpha\beta}$ for $\tau = 0$

$$\begin{aligned} \left. \frac{\partial c_{\alpha\beta}}{\partial \tau} \right|_{\tau=0} &= \int (R - R_0)_{\alpha} (R - R_0)_{\beta} \left. \frac{\partial G}{\partial \tau}(\mathbf{R}, \mathbf{R}_0, \tau) \right|_{\tau=0} d\mathbf{R} \\ &= -\Psi_T^{-1}(\mathbf{R}_0) \int (R - R_0)_{\alpha} (R - R_0)_{\beta} \Psi_T(\mathbf{R}) \langle \mathbf{R}_0 | \hat{H}^{PS} | \mathbf{R} \rangle d\mathbf{R} \\ &= -\Psi_T^{-1}(\mathbf{R}_0) \int \delta(\mathbf{R} - \mathbf{R}_0) \hat{H}^{PS} [(R - R_0)_{\alpha} (R - R_0)_{\beta} \Psi_T(\mathbf{R})] d\mathbf{R}, \end{aligned} \quad (8)$$

where in the last lines we have used the fact that \hat{H}^{PS} is Hermitian and that we can always choose real wave functions. Using repeatedly the relation

$$[R_\alpha, f(\hat{P})] = i \frac{\partial f}{\partial \hat{P}_\alpha}, \quad (9)$$

we end up with

$$\begin{aligned} \left. \frac{\partial c_{\alpha\beta}}{\partial \tau} \right|_{\tau=0} &= \Psi_T^{-1}(\mathbf{R}_0) \int \delta(\mathbf{R} - \mathbf{R}_0) \frac{\partial^2 \hat{H}^{PS}}{\partial \hat{P}_\alpha \partial \hat{P}_\beta} \Psi_T(\mathbf{R}) \\ &= \Psi_T^{-1}(\mathbf{R}_0) \left[\frac{\partial^2 \hat{H}^{PS}}{\partial \hat{P}_\alpha \partial \hat{P}_\beta} \Psi_T(\mathbf{R}) \right]_{\mathbf{R}=\mathbf{R}_0}. \end{aligned} \quad (10)$$

This expression can be chosen positive definite for each trial function Ψ_T only if \hat{H}^{PS} is of the form

$$\begin{aligned} \hat{H}^{PS} &= W(\mathbf{R}) + \sum_{\alpha=1}^{3N} K_\alpha(\mathbf{R}) \hat{P}_\alpha \\ &+ \sum_{\alpha,\beta=1}^{3N} T_{\alpha\beta}(\mathbf{R}) \hat{P}_\alpha \hat{P}_\beta, \end{aligned} \quad (11)$$

whence

$$\begin{aligned} \left. \frac{\partial c_{\alpha\beta}}{\partial \tau} \right|_{\tau=0} &= \Psi_T^{-1}(\mathbf{R}_0) T_{\alpha\beta}(\mathbf{R}_0) \Psi_T(\mathbf{R}_0) \\ &= T_{\alpha\beta}(\mathbf{R}_0). \end{aligned} \quad (12)$$

In conclusion, the local Hamiltonian to be used with GFMC must have the form of Eq. (11), with the Hessian tensor $T_{\alpha\beta}(\mathbf{R}_0)$ positive definite for each $\mathbf{R}_0 \in D$. This guarantees that $\partial c_{\alpha\beta}(\mathbf{R}_0, \tau)/\partial \tau$ and $c_{\alpha\beta}(\mathbf{R}_0, \tau)$ are also positive definite $\forall \mathbf{R}_0 \in D$ in a right neighborhood of $\tau = 0$, and consequently it is a necessary condition to have $G(\mathbf{R}, \mathbf{R}', \tau)$ non-negative in the same neighborhood. This rules out a large number of conceivable local Hamiltonians \hat{H}^{PS} , in particular those containing any power of momentum higher than 2. If we further require the two following conditions to hold:

(a) that \hat{H}^{PS} has the same structure of the true Hamiltonian for a collection of spherically symmetric atoms,

$$\begin{aligned} \hat{H}^{PS} &= -\frac{1}{2} \sum_i \nabla_i^2 + \frac{1}{2} \sum_{i,j \neq i} \frac{1}{r_{ij}} + \sum_{i,I} \hat{v}_I^{PS}(r_{iI}) \\ &= \sum_i \hat{h}_i^{PS} + \frac{1}{2} \sum_{i,j \neq i} \frac{1}{r_{ij}}, \end{aligned} \quad (13)$$

where i, j run over valence electrons, I runs over ions, $r_{ij} = |\mathbf{r}_i - \mathbf{r}_j|$, $r_{iI} = |\mathbf{r}_i - \mathbf{s}_I|$, $\{\mathbf{r}_i\}$ are the electronic coordinates, $\{\mathbf{s}_I\}$ the ionic coordinates, and \hat{v}_I^{PS} describes the electronic interaction with the I th ion;

(b) that \hat{H}^{PS} be invariant against time-reversal symmetry [21],

then we end up, for one electron in the field of one ion, with the pseudo-Hamiltonian [10]

$$\hat{h}^{PS} = -\frac{1}{2} \nabla [A(r) + 1] \nabla + \frac{B(r)}{2r^2} \hat{L}^2 + v_{ion}(r), \quad (14)$$

and the conditions

$$\begin{aligned} A(r) + 1 &> 0, \\ A(r) + B(r) + 1 &> 0, \end{aligned} \quad (15)$$

which guarantee that \hat{h}^{PS} is bounded from below. Going back to Cartesian coordinates with all the derivatives on the right, we have

$$\begin{aligned} \hat{h}^{PS} &= -\frac{1}{2} \sum_{\alpha,\beta=1}^3 \left\{ [A(r) + B(r) + 1] \delta_{\alpha\beta} - \frac{B(r)}{r^2} r_\alpha r_\beta \right\} \\ &\times \frac{\partial}{\partial r_\alpha} \frac{\partial}{\partial r_\beta} \\ &+ \sum_{\alpha=1}^3 \left[-\frac{A'(r)}{2} + \frac{B(r)}{r} \right] \frac{r_\alpha}{r} \frac{\partial}{\partial r_\alpha} + v_{ion}(r), \end{aligned} \quad (16)$$

which can be proved to produce a Green's function $G(\mathbf{r}, \mathbf{r}', \tau)$ whose leading term in the short time approximation is non-negative [22].

B. The Kohn-Sham equations

We are now going to write down the Kohn-Sham equations within the DFT-LDA for both the full-core Hamiltonian and the pseudo-Hamiltonian in the spherical approximation (the Appendix gives details about their solution). Let $\epsilon_{n\ell}$ and $\chi_{n\ell}(r)$ be the single-particle eigenvalues and radial eigenfunctions of angular momentum ℓ and of quantum number n (in the following n will be dropped, since for each angular momentum ℓ we focus only on one valence state), and denote the full-core quantities with the upper index FC (this notation will be used throughout the paper). We have then

$$\begin{aligned} -\frac{1}{2} \frac{d^2 \chi_{n\ell}^{FC}(r)}{dr^2} + \left[\frac{\ell(\ell+1)}{2r^2} - \frac{Z}{r} + v_{HXC}^{FC}(r) \right] \chi_{n\ell}^{FC}(r) \\ = \epsilon_{n\ell}^{FC} \chi_{n\ell}^{FC}(r), \end{aligned} \quad (17)$$

$$\begin{aligned} -\frac{1}{2} [A(r) + 1] \frac{d^2 \chi_{n\ell}(r)}{dr^2} + \left\{ [A(r) + B(r) + 1] \frac{\ell(\ell+1)}{2r^2} \right. \\ \left. - \frac{1}{2} \frac{dA}{dr} \left[\frac{d}{dr} - \frac{1}{r} \right] + v_{ion}(r) + v_{HXC}(r) \right\} \chi_{n\ell}(r) \\ = \epsilon_{n\ell} \chi_{n\ell}(r). \end{aligned} \quad (18)$$

When relativistic effects are important, we replace Eq. (17) with a scalar-relativistic Dirac equation [24]. $v_{HXC}(r)$ is the Hartree, exchange, and correlation potential defined as

$$v_{HXC}(r) = \int \frac{n(r')}{|\mathbf{r} - \mathbf{r}'|} d^3 \mathbf{r}' + \frac{\delta E_{XC}^{LDA}[n]}{\delta n(r)}, \quad (19)$$

$$n(r) \equiv \frac{1}{4\pi r^2} \sum_{n\ell} f_{n\ell} |\chi_{n\ell}(r)|^2. \quad (20)$$

$E_{XC}^{LDA}[n]$ is the DFT-LDA exchange-correlation energy functional [25,26], $n(r)$ the charge density, and $f_{n\ell}$ the occupation numbers of the Kohn-Sham radial orbitals $\chi_{n\ell}(r)$ [14]. To simplify the notation, we introduce the functions $a(r)$, $c(r)$, and $v(r)$, defined as follows:

$$a(r) = A(r) + 1, \quad (21a)$$

$$c(r) = A(r) + B(r) + 1, \quad (21b)$$

$$v(r) = v_{ion}(r) + v_{HXC}(r), \quad (21c)$$

$$v^{FC}(r) = -\frac{Z}{r} + v_{HXC}^{FC}(r). \quad (21d)$$

Then Eq. (18) becomes

$$\begin{aligned} \frac{1}{2} \int_0^{+\infty} \chi_\ell(r) \frac{d}{dr} \left[a(r) \frac{d\chi_{\ell'}}{dr}(r) \right] dr - \frac{1}{2} \int_0^{+\infty} \chi_{\ell'}(r) \frac{d}{dr} \left[a(r) \frac{d\chi_\ell}{dr}(r) \right] dr \\ + \frac{1}{2} [\ell(\ell+1) - \ell'(\ell'+1)] \int_0^{+\infty} c(r) \frac{\chi_\ell(r)\chi_{\ell'}(r)}{r^2} dr = (\epsilon_\ell - \epsilon_{\ell'}) \int_0^{+\infty} \chi_\ell(r)\chi_{\ell'}(r) dr. \end{aligned} \quad (23)$$

Rearranging the first term on the left

$$\begin{aligned} \int_0^{+\infty} \chi_\ell(r) \frac{d}{dr} \left[a(r) \frac{d\chi_{\ell'}}{dr}(r) \right] dr &= \left[\chi_\ell(r) a(r) \frac{d\chi_{\ell'}}{dr}(r) \right]_0^{+\infty} - \int_0^{+\infty} \frac{d\chi_\ell}{dr}(r) a(r) \frac{d\chi_{\ell'}}{dr}(r) dr \\ &= - \left[\frac{d\chi_\ell}{dr}(r) a(r) \chi_{\ell'}(r) \right]_0^{+\infty} + \int_0^{+\infty} \chi_{\ell'}(r) \frac{d}{dr} \left[a(r) \frac{d\chi_\ell}{dr}(r) \right] dr \\ &= \int_0^{+\infty} \chi_{\ell'}(r) \frac{d}{dr} \left[a(r) \frac{d\chi_\ell}{dr}(r) \right] dr, \end{aligned} \quad (24)$$

where we have used the fact that $\chi_\ell(0) = 0$ and $\chi_\ell(+\infty) = 0$ (see the Appendix), Eq. (23) becomes

$$\begin{aligned} (\epsilon_\ell - \epsilon_{\ell'}) \int_0^{+\infty} \chi_\ell(r)\chi_{\ell'}(r) dr \\ = \frac{1}{2} [\ell(\ell+1) - \ell'(\ell'+1)] \int_0^{+\infty} c(r) \frac{\chi_\ell(r)\chi_{\ell'}(r)}{r^2} dr. \end{aligned} \quad (25)$$

$c(r)$ is positive for each $r > 0$, and if we take for χ_ℓ and $\chi_{\ell'}$ the lowest energy states of angular momentum ℓ and ℓ' , which are nodeless and can be chosen real and positive $\forall r > 0$, it follows that

$$\epsilon_\ell > \epsilon_{\ell'} \Leftrightarrow \ell > \ell' \quad \forall \ell, \ell', \quad (26)$$

which gives the ordering rule [11] which limits the pseudo-Hamiltonian method to sp -bonded systems [12].

C. Norm conservation

Now we are ready to generalize the method of Ref. [9] for the construction of pseudo-Hamiltonians. We start from a reference atomic state containing all the orbitals whose angular momentum is relevant for the va-

$$\begin{aligned} -\frac{1}{2} a(r) \frac{d^2 \chi_\ell(r)}{dr^2} + \left\{ c(r) \frac{\ell(\ell+1)}{2r^2} \right. \\ \left. - \frac{1}{2} \frac{da}{dr} \left[\frac{d}{dr} - \frac{1}{r} \right] + v(r) \right\} \chi_\ell(r) = \epsilon_\ell \chi_\ell(r). \end{aligned} \quad (22)$$

As already briefly mentioned in the Introduction, Foulkes and Schlüter have shown that our operator necessarily yields a “natural” order $\epsilon_s \leq \epsilon_p \leq \epsilon_d \leq \dots$ of the energy eigenvalues [11]. It may be useful, based on Eq. (22), to recall their point in greater detail now. If we multiply Eq. (22) by $\chi_{\ell'}(r)$ on the left, subtract it from itself after the exchange of ℓ with ℓ' , and integrate the result from $r = 0$ to $+\infty$, we obtain

lence systems we are interested in. This is one of the main differences from nonlocal pseudopotentials: we need all angular momenta in one shot because the pseudo-Hamiltonian, being local, acts on all angular momenta at the same time, rather than picking them one by one as a typical Hamann-Schlüter-Chiang nonlocal potential does through projection operators. In practice $\ell = 0, 1$ (s and p waves) or $\ell = 0, 1, 2$ (s , p , and d waves) are enough to characterize most of the interesting elements of the periodic table [27]. We choose a single core radius r_c , the same for each of the three functions $a(r)$, $c(r)$, and $v(r)$, and use it in a way more similar to Kerker [28] than to Hamann, Schlüter, and Chiang [9]. Given the reference state and the core radius we can write the four main requirements for our pseudo-Hamiltonian; three of them are just identical to the procedure of Ref. [9]; the fourth is peculiar to our pseudo-Hamiltonian:

- (1) identical full-core and pseudo-single-particle valence eigenvalues ($P1$);
- (2) correctly normalized pseudo-single-particle valence orbitals which are identical to the full-core orbitals outside the core (norm conservation) ($P2$);
- (3) valence orbitals without nodes ($P3$);
- (4) “positivity” conditions: $A(r) + 1 > 0$ and $A(r) + B(r) + 1 > 0$ ($P4$).

An immediate consequence of the property ($P3$) is that for each angular momentum ℓ our valence orbital is the

lowest energy eigenstate of Eq. (22). This also shows that nothing can be done to beat the ordering rule, Eq. (26): the only ways around it are either to drop the property (P3), which would introduce unphysical pseudocore states, or to drop the condition (P4) [$c(r) > 0 \forall r > 0$], which, instead, would violate the fixed-node GFMC requirements and make the energy spectrum of \hat{h}^{PS} unbounded from below. Therefore the ordering rule first pointed out by Foulkes and Schlüter [11] poses a severe limitation on the description of transition elements for which the energy ordering of valence states seldom follows Eq. (26): in this case the true valence-only atom cannot be reproduced by any pseudo-Hamiltonian satisfying the properties (P1) to (P4).

The properties (P1) and (P2) imply the following asymptotic behavior for $a(r)$, $c(r)$, and $v(r)$:

$$\left. \begin{array}{l} a(r) = 1 \\ c(r) = 1 \\ v(r) = v^{FC}(r) \end{array} \right\} \quad \forall r \geq r_c. \quad (27)$$

In analogy with the method of Hamann, Schlüter, and Chiang [9], it can be shown that the properties (P1) and (P2) imply the equality of full-core and pseudologarithmic derivatives of the single-particle wave functions to first order in energy. If we proceed in a way similar to that described in Ref. [9], but using Eq. (22) for the pseudo-Hamiltonian, we end up with

$$\left. \frac{\partial x_\ell(\epsilon, r)}{\partial \epsilon} \right|_{r=R} = -\frac{2}{a(R)\chi_\ell^2(\epsilon, R)} \int_0^R \chi_\ell^2(\epsilon, r) dr, \quad (28)$$

$$x_\ell(\epsilon, r) \equiv \frac{\chi'_\ell(\epsilon, r)}{\chi_\ell(\epsilon, r)}, \quad (29)$$

where $\chi_\ell(\epsilon, r)$ is the solution of the radial Schrödinger Eq. (22), which is regular in $r = 0$ and corresponds to the single-particle energy ϵ , in some reference state (usually the atomic ground state), $\chi'_\ell(\epsilon, r)$ its first derivative with respect to r and $x_\ell(\epsilon, r)$ its logarithmic derivative (see the Appendix). For $R > r_c$, since $a(R) = 1$, Eq. (28) reduces to the well known result [9,29]

$$\left. \frac{\partial x_\ell(\epsilon, r)}{\partial \epsilon} \right|_{r=R} = -\frac{2}{\chi_\ell^2(\epsilon, R)} \int_0^R \chi_\ell^2(\epsilon, r) dr, \quad (30)$$

and hence, as originally shown by Hamann, Schlüter, and Chiang [9], the “norm conservation” [properties (P1) and (P2)] is of key importance for the ionic transferability. While Eq. (30), for $R > r_c$, holds both for pseudo-Hamiltonians and nonlocal pseudopotentials, this is not true for higher order logarithmic-derivative energy derivatives. Shirley *et al.* [29] have obtained for nonlocal pseudopotentials

$$\begin{aligned} & \left(\frac{\partial}{\partial \epsilon} \right)^n x_\ell(\epsilon, r) \Big|_{r=R} \\ &= -\frac{1}{\chi_\ell^2(\epsilon, R)} \sum_{i=1}^{n-1} \binom{n}{i} \int_0^R \chi_\ell^2(\epsilon, r) \left(\frac{\partial}{\partial \epsilon} \right)^i \\ & \quad \times x_\ell(\epsilon, r) \left(\frac{\partial}{\partial \epsilon} \right)^{n-i} x_\ell(\epsilon, r) dr, \end{aligned} \quad (31)$$

while Lastri [30] has shown that for the pseudo-Hamiltonian these quantities are equal to

$$\begin{aligned} & \left(\frac{\partial}{\partial \epsilon} \right)^n x_\ell(\epsilon, r) \Big|_{r=R} \\ &= -\frac{1}{\chi_\ell^2(\epsilon, R)} \sum_{i=1}^{n-1} \binom{n}{i} \int_0^R a(r) \chi_\ell^2(\epsilon, r) \left(\frac{\partial}{\partial \epsilon} \right)^i \\ & \quad \times x_\ell(\epsilon, r) \left(\frac{\partial}{\partial \epsilon} \right)^{n-i} \\ & \quad \times x_\ell(\epsilon, r) dr. \end{aligned} \quad (32)$$

Equation (32) differs from Eq. (31) in the presence of $a(r)$ under the integral sign; this is a way to see why, even if a pseudo-Hamiltonian and a pseudopotential have identical pseudo-wave-functions at some reference energy ϵ_ℓ , their logarithmic derivatives, for energies away from the reference state, will sooner or later disagree [31].

D. Pseudo-Hamiltonian and nonlocal pseudopotentials

In this section we consider the relationship between the pseudo-Hamiltonian and nonlocal pseudopotentials in the DTF-LDA framework. If we compare the Kohn-Sham equation (18) for the pseudo-Hamiltonian with the corresponding one for nonlocal pseudopotentials

$$-\frac{1}{2} \frac{d^2 \chi_\ell(r)}{dr^2} + \left[\frac{\ell(\ell+1)}{2r^2} + v_\ell^{PS}(r) + v_{HXC}(r) \right] \chi_\ell(r) = \epsilon_\ell \chi_\ell(r), \quad (33)$$

and we require that both of them have the same eigenvalues ϵ_ℓ and eigenvectors $\chi_\ell(r)$ for $\ell = 0, 1, 2$, by subtraction we obtain the following equation linking $A(r)$, $B(r)$, and $v_{ion}(r)$ with $v_\ell^{PS}(r)$:

$$\begin{aligned} & A(r) \frac{1}{\chi_\ell(r)} \frac{d^2 \chi_\ell(r)}{dr^2} - [A(r) + B(r)] \frac{\ell(\ell+1)}{2r^2} \\ & + \frac{dA}{dr} \left[\frac{1}{\chi_\ell(r)} \frac{d\chi_\ell(r)}{dr} - \frac{1}{r} \right] + 2[v_\ell^{PS}(r) - v_{ion}(r)] = 0. \end{aligned} \quad (34)$$

We notice that the role of the six potentials is not symmetric: given $A(r)$, $B(r)$, and $v_{ion}(r)$ there are no difficulties in calculating the corresponding $v_\ell^{PS}(r)$, while given the latter we must solve a first-order differential equation to obtain $A(r)$ [10,11],

$$G(r)A' + F(r)A + 2V(r) = 0, \quad (35)$$

where $G(r)$, $F(r)$, and $V(r)$ are functions involving $v_\ell^{PS}(r)$, $\chi_\ell(r)$, and ϵ_ℓ . This equation must be solved with the initial condition $A(r_c) = 0$. Unfortunately, experience tells us that two main difficulties arise when trying to solve for $A(r)$ using standard nonlocal pseudopotentials [33]: either $G(r)$ has some zeros in $[0, r_c]$

and $A'(r)$ diverges in such points, or the property (P4) is not satisfied. Since nonlocal pseudopotentials are by no means unique inside the core, it was initially hoped that small norm-conserving distortions of existing nonlocal pseudopotentials might remove these two obstacles and make the use of Eqs. (34) and (35) a viable route to the construction of pseudo-Hamiltonians from nonlocal pseudopotentials. Again experience has soon shown that this was not a realistic hope: “in the neighborhood” of existing nonlocal pseudopotentials there is no good solution to Eqs. (34) and (35) which satisfies all the required constraints, and thus no acceptable pseudo-Hamiltonians [10]. The way Bachelet, Ceperley, and Chiochetti [10] went around this problem was to avoid the differential Eq. (35) by dropping $\ell = 2$, thus reducing to $\ell = 0, 1$. Of course an sp -only pseudoion is less accurate than an spd pseudoion, but transition metals are out of reach anyway, and for the remainder of the periodic table (sp elements) the lack of d -wave nonlocality is not too serious. This leaves $A(r)$ undetermined and we can parametrize it by means of A_0 , r_0 , and k ,

$$A(r) = A_0 \exp \left[- \left(\frac{r}{r_0} \right)^k \right], \quad r_0, k > 0; \quad (36)$$

based on any such $A(r)$ we then explicitly derive $B(r)$ and $v_{ion}(r)$ from the $\ell = 0$ and $\ell = 1$ pseudopotentials and pseudo-wave-functions through Eq. (34), and finally try to fix the three parameters A_0 , r_0 , and k in such a way as to fulfill the property (P4). This method has proven to work for a number of simple sp elements [10]. Of course the d wave is poorly described and, even in the cases where only s and p waves are relevant, if one does not pay attention, a too tightly bound d state can lead to unphysical effects.

The idea of focusing on two wave functions χ_0 and χ_1 and working on $A(r)$ has been generalized and pursued by Foulkes and Schlüter [11]. They do not start from nonlocal pseudopotentials, but directly parametrize in a suitable and efficient way these three functions, and optimize the parameters in such a way as to satisfy the property (P4) and the properties (P1) and (P2) for χ_2 and ϵ_2 ; ϵ_0 , and ϵ_1 satisfy the property (P1) and are kept fixed.

III. CONSTRUCTION TECHNIQUE

A. Fundamentals

We are now going to consider in greater detail all the desired properties for the pseudo-Hamiltonian, which have been stated in Sec. II C. We can group these properties according to two different criteria. A first distinction can be made between main requirements and secondary ones. The former are those conditions which must be exactly satisfied for the pseudo-Hamiltonian to have physical meaning as a valence-only norm-conserving Hamiltonian. The latter are additional conditions and can be fulfilled only approximately: the degree of fulfillment will measure the quality of the pseudo-Hamiltonian (from the point of view of its possible use in a wider and wider range

of different physical systems). A second distinction is possible in connection with the details of our construction: some requirements will be satisfied by construction or by restricting the domain in the space of the Hermitian operators that we are searching (built-in requirements), while others will be obtained by a stepwise numerical optimization scheme.

Using the same notation of Sec. II, we can write the properties (P1) to (P4) outlined in Sec. II C as

$$\epsilon_\ell = \epsilon_\ell^{FC}, \quad \ell = 0, 1, 2, \quad (37)$$

$$\chi_\ell(r) = \chi_\ell^{FC}(r), \quad \forall r \geq r_c, \quad (38)$$

$$\int_0^{r_c} |\chi_\ell(r)|^2 dr = \int_0^{r_c} |\chi_\ell^{FC}(r)|^2 dr, \quad (39)$$

$$\chi_\ell(r) \neq 0, \quad \forall r > 0, \quad (40)$$

$$a(r) > 0, \quad (41)$$

$$c(r) > 0.$$

In addition, to guarantee that the operator \hat{h}^{PS} of Eq. (16) is defined for $r = 0$, we must have

$$\lim_{r \rightarrow 0} B(r) = 0, \quad (42)$$

$$\lim_{r \rightarrow 0} \left[-\frac{A'(r)}{2} + \frac{B(r)}{r} \right] = 0, \quad (43)$$

which are satisfied if we choose

$$A'(r) \stackrel{r \rightarrow 0}{\sim} O(r), \quad (44)$$

$$\frac{B(r)}{r} \stackrel{r \rightarrow 0}{\sim} O(r). \quad (45)$$

Consequently [30,34]

$$\begin{aligned} a(r) &= a_0 + a_1 r + O(r^2), \\ c(r) &= c_0 + c_1 r + O(r^2), \end{aligned} \quad (46)$$

$$a_0 = c_0,$$

$$a_1 = c_1 = 0.$$

The reason why in Eqs. (44) and (45) we take $O(r)$ and not a fractional power of r is the fact that $r = 0$ is a singular point for Eq. (22); our choice guarantees that this singular point is “regular” [35] and the equation admits two linearly independent solutions, one of which is finite for $r = 0$ (see the Appendix). If $v(r)$ is finite for $r = 0$, it is easy to show that $a_0 = c_0$ and $a_1 = c_1 = 0$ if and only if [34]

$$\chi_\ell(r) \stackrel{r \rightarrow 0}{\sim} O(r^{\ell+1}) + O(r^{\ell+3}), \quad (47)$$

where $O(r^{\ell+1})$ is also the first term in the expansion near $r = 0$ of the LDA wave functions of the full-core atom and of the nonlocal pseudopotentials; the next term in the

expansion of the full-core wave function is $O(r^{\ell+2})$ due to the Coulombic singularity of the nuclear potential, while for nonlocal pseudopotentials we have again $O(r^{\ell+3})$.

Equations (37)–(41) and Eqs. (46) are the main requirements. In our approach, due to the difficulty of imposing constraints expressed by inequalities, Eq. (41) is treated as a built-in condition, together with Eq. (46) [see below Eq. (50)]; Eq. (38) too (exact matching with the full-core atom outside the core is also built in); Eqs. (37), (39), and (40) are instead imposed by a numerical optimization scheme. Secondary requirements arise from practical reasons [36]. These take us to consider only those radial functions $a(r)$, $c(r)$, and $v(r)$ which are bounded and continuous with their first derivatives $\forall r \geq 0$. As far as the matching properties of $a(r)$, $c(r)$, and $v(r)$ with the known expressions outside the core radius r_c are concerned, we explicitly require the continuity of the functions and their first derivatives at r_c (built in, see Sec. III C)

$$\begin{aligned} a(r_c) &= 1, \\ a'(r_c) &= 0, \\ c(r_c) &= 1, \\ c'(r_c) &= 0, \\ v(r_c) &= v^{FC}(r_c), \\ v'(r_c) &= v'^{FC}(r_c), \end{aligned} \quad (48)$$

where $v^{FC}(r)$ is the full-core self-consistent potential.

While Eq. (41) fixes only a lower bound on $a(r)$ and $c(r)$, several reasons suggest imposing more stringent bounds on them. Too wide a variation of these functions in the range $[0, r_c]$ can give numerical problems connected with the use of the pseudo-Hamiltonian in real calculations; too large or too small values of $a(r)$ and $c(r)$ over a substantial fraction of $[0, r_c]$ can change the effects of the kinetic energy operator and the centrifugal potential on the single-particle LDA wave functions in such a way as to push abnormally up or down in energy the excited states, thus deteriorating the transferability of the pseudo-Hamiltonian. We then choose

$$\begin{aligned} 0 < a_{lo} \leq a(r) \leq a_{hi}, \\ 0 < c_{lo} \leq c(r) \leq c_{hi}. \end{aligned} \quad (49)$$

The lower bounds, which imply Eq. (41), will be a built-in condition, while the upper bounds will be obtained by a stepwise minimization.

The group of Eqs. (48) and (49) yield a smooth matching at r_c and avoid huge variations of $a(r)$, $c(r)$, and $v(r)$, but do not tell anything about their smoothness, which is a desirable property for most practical applications. To accomplish this goal we build an optimally smooth function over the interval $[0, r_c]$ as a linear combination of certain special functions $\{R_i\}$ with coefficients $\{\lambda_i\}$ (Sec. III C). In this way, keeping in mind both Eqs. (41) and Eq. (49), our “smoothness” requirement can be turned into the built-in condition

$$\left. \begin{aligned} a(r) &= a_{lo} + [\sum_i \lambda_i^a R_i(r)]^2 \\ c(r) &= c_{lo} + [\sum_i \lambda_i^c R_i(r)]^2 \\ v(r) &= \sum_i \lambda_i^v R_i(r) \end{aligned} \right\}, \quad r \in [0, r_c]. \quad (50)$$

The Eqs. (46) and (48), in conjunction with the previous expressions, introduce linear relations among the coefficients $\{\lambda_i^a\}$, $\{\lambda_i^c\}$, and $\{\lambda_i^v\}$ of Eqs. (50).

Additional conditions can be thought and conceived [37]. For example, we have sometimes added the request of improved logarithmic derivatives beyond the usual norm conservation [9,38]. We obtained that by choosing for every state of angular momentum ℓ a second energy ϵ'_ℓ above the corresponding eigenvalue ϵ_ℓ ($\epsilon'_\ell > \epsilon_\ell$) and, as a secondary condition (to be obtained by numerical stepwise minimization), required the matching of full-core and pseudologarithmic derivatives also at this second energy ϵ'_ℓ , i.e., required the following equality to hold for $R = r_c$:

$$\frac{\chi'_\ell(\epsilon'_\ell, R)}{\chi_\ell(\epsilon'_\ell, R)} = \frac{\chi'^{FC}_\ell(\epsilon'_\ell, R)}{\chi^{FC}_\ell(\epsilon'_\ell, R)}, \quad (51)$$

$\chi^{FC}_\ell(\epsilon, r)$ and $\chi_\ell(\epsilon, r)$, being the eigensolutions of the radial Schrödinger Eqs. (17) and (22) which correspond to the energy ϵ , are regular in the origin $r = 0$, and are, in general, not normalizable [30]. The self-consistent potential, Eqs. (21c) and (21d), is that of the reference state (Appendix).

B. The cost functional and its minimization

Our distinction between conditions which are built in and conditions to be imposed by numerical stepwise minimization has no physical relevance, and is by no means unique. It just simplifies the problem of constructing a suitable pseudo-Hamiltonian for a given element in terms of the algorithm to be implemented on a computer. The problem of determining $a(r)$, $c(r)$, and $v(r)$ is highly nonlinear because these three functions are linked to the properties of the original full-core atom via the second-order eigenvalue differential Eq. (22) and the conditions appearing in Eqs. (37), (39), and (40) [plus, possibly, Eq. (51)]. An additional difficulty comes from Eq. (41), the most difficult constraint which prohibited [10] the straightforward use of nonlocal norm-conserving pseudopotentials [33] to generate the pseudo-Hamiltonian by direct inversion of Eq. (34). Precisely because of this experience we decided that the best strategy is to have this condition automatically verified at the very start, i.e., to include it among the built-in conditions. The built-in conditions are analytically implemented in a very simple way which will be detailed later on. Here, instead, we want to illustrate how those equalities or inequalities which are not built in can be approached by a numerical stepwise minimization. Fortunately also for this second purpose there is a relatively simple and natural way: one only needs to reasonably quantify the degree of approximation in fulfilling an equality or an inequality. If the equation $x = y$ holds only approximately, then the “distance”

$$d(x, y) = (x - y)^2 \geq 0 \quad (52)$$

can be a practical measure of the deviation from the equality [satisfied exactly if and only if $d(x, y) = 0$] and

can be generalized for the inequality $x \geq y$ as

$$D(x, y) = (x - y)^2 \theta(y - x) \geq 0, \quad (53)$$

where θ is the Heaviside function or, if x and y are functions defined over the interval $[a, b]$,

$$D(x, y) = \int_a^b [x(r) - y(r)]^2 \theta(y(r) - x(r)) dr \geq 0. \quad (54)$$

If we sum all the so-defined “distances” for Eqs. (37), (39), (40), and (49) and Eq. (51), we obtain a functional of $a(r)$, $c(r)$, and $v(r)$ which is non-negative, and equals zero if and only if the equations hold exactly, that is, a functional whose absolute minimum zero, if it exists, corresponds to our ideal pseudo-Hamiltonian. Even if the functional never takes the value zero (or we are not able to find it), it remains true that the lower the value we can find, the better approximation to the exact solution we have reached. In fact, a straight sum of the “distances” in the definition of the functional as suggested by Eqs. (52)–(54) may not be the best idea. A weighted sum of these distances will take care of their absolute magnitude and of their importance (main vs secondary requirements) in a controlled way, and we thus prefer this choice. We then define our cost functional as follows:

$$\begin{aligned} E_{cost}[a, c, v] &= E_{eig}[a, c, v] + E_{norm}[a, c, v] \\ &\quad + E_{node}[a, c, v] + E_{bound}[a, c, v] \\ &\quad + E_{id}[a, c, v], \end{aligned} \quad (55)$$

$$E_{eig}[a, c, v] = \sum_{\ell=0}^2 \beta_{\ell} d[x_{\ell}(\epsilon_{\ell}^{FC}, r_c), x_{\ell}^{FC}(\epsilon_{\ell}^{FC}, r_c)], \quad (56a)$$

$$E_{norm}[a, c, v] = \sum_{\ell=0}^2 \gamma_{\ell} d(N_{\ell}, N_{\ell}^{FC}), \quad (56b)$$

$$E_{node}[a, c, v] = \begin{cases} 0 & \text{if } \chi_{\ell}(r) \neq 0 \quad \forall r > 0 \\ +\infty & \text{otherwise,} \end{cases} \quad (56c)$$

$$E_{bound}[a, c, v] = \eta D(a_{hi}, a) + \mu D(c_{hi}, c), \quad (56d)$$

$$E_{id}[a, c, v] = \sum_{\ell=0}^2 \delta_{\ell} d[x_{\ell}(\epsilon'_{\ell}, r_c), x_{\ell}^{FC}(\epsilon'_{\ell}, r_c)], \quad (56e)$$

where

$$N_{\ell} = \int_0^{r_c} |\chi_{\ell}(\epsilon_{\ell}^{FC}, r)|^2 dr, \quad (57)$$

and β_{ℓ} , γ_{ℓ} , δ_{ℓ} , η , and μ weight the importance of the corresponding terms. The various contributions to the cost functional E_{cost} correspond to and are listed in the same order as Eqs. (37), (39), (40), and (49) and Eq. (51). $d[x_{\ell}(\epsilon_{\ell}^{FC}, r_c), x_{\ell}^{FC}(\epsilon_{\ell}^{FC}, r_c)]$ is equivalent to $d(\epsilon_{\ell}, \epsilon_{\ell}^{FC})$ because $x_{\ell}(\epsilon_{\ell}^{FC}, r_c) = x_{\ell}^{FC}(\epsilon_{\ell}^{FC}, r_c) \Leftrightarrow \epsilon_{\ell} = \epsilon_{\ell}^{FC}$, but to determine the eigenvalue ϵ_{ℓ} implies much more work than to obtain $x_{\ell}(\epsilon_{\ell}^{FC}, r_c)$ [the latter task requires just one more integration of Eq. (22) from $r = 0$ to $r = r_c$; see the Appendix]. Equation (40) has been taken into account with the accept-reject term E_{node} : only a , c , and v such that $\chi_{\ell}(r) \neq 0 \quad \forall r > 0$ are accepted.

Since, through Eqs. (50), a , c , and v are now functions of $\{\lambda_i^a\}$, $\{\lambda_i^c\}$, and $\{\lambda_i^v\}$ (the next subsection contains all the details of our basis set), the functional E_{cost} is also turned into a function of $\{\lambda_i^a\}$, $\{\lambda_i^c\}$, and $\{\lambda_i^v\}$, and as such it is used in practice: one looks for the minimum of E_{cost} in the multidimensional space of $\{\lambda_i^a\}$, $\{\lambda_i^c\}$, and $\{\lambda_i^v\}$. Neither theoretical reasons nor experience suggest that this cost function is unimodal (without local minima). For a multimodal function of many variables, unless we know with enough accuracy the position of the absolute minimum, we are faced with the problem of avoiding local minima during the search of the global minimum. Many deterministic algorithms are available which, given a certain starting point, will rapidly locate the closest local minimum of the target function [39], but our problem is that here we do not have in advance a good starting point. If we only rely on deterministic algorithms, we should then try very many (in principle infinite) different starting points at random, obtain by deterministic search many (all) local minima, and finally select the best one (in principle the absolute minimum). This is, however, impractical if the number of variables is high. A much more efficient approach is the simulated annealing with Metropolis Monte Carlo sampling [40–44] in which a random walk in the domain of search is supported by a sampling criterion that drives the walk only into the most interesting regions, and in such a way as to avoid trapping in the various local minima. The idea of using simulated annealing to generate pseudo-Hamiltonians is due to Mitáš and co-workers [20,45], who also demonstrated the feasibility of this approach. The global minimum is reached with unit probability only for an infinite walk [42] but, if we fix a threshold (above the ideal value of zero) corresponding to an acceptable approximation for the pseudo-Hamiltonian, we often reach a region where the cost function is below our desired accuracy within a reasonable amount of time (or length of the walk) [46]. In practice the simulated annealing procedure is stopped as soon as the cost function goes below the threshold; we found it convenient to use a nonlinear simplex method [39] to improve the minimum found as the ending point of the simulated annealing and thus obtain the final optimal solution.

C. Representation of $a(r)$, $c(r)$, and $v(r)$

As we have anticipated in the preceding section, a numerical approach is feasible if we can treat in a convenient finite form the three continuous functions $a(r)$, $c(r)$, and $v(r)$ and thus turn the cost functional into a function of a finite number of variables. An obvious possibility is to expand each of the three functions a , c , and v in terms of some suitable finite basis set, and then to work with the coefficients $\{\lambda_i^a\}$, $\{\lambda_i^c\}$, and $\{\lambda_i^v\}$ of such an expansion. Many analytical basis sets are available; among them we have chosen a nonorthogonal family $\{R_i\}$, the regularized splines with tension (RST), whose main virtue, in our view, is its smoothness criterion [47,48]. In Eq. (50) as given in Sec. III A, we take

$$\left. \begin{aligned} R_0(x) &= 1 \\ R_i(x) &= R(x, x_i) \\ R_{N+1}(x) &= \left. \frac{\partial}{\partial y} R(x, y) \right|_{y=x_N} \\ R_{N+2}(x) &= \left. \frac{\partial}{\partial y} R(x, y) \right|_{y=x_1} \end{aligned} \right\} \quad i = 1, \dots, N. \quad (58)$$

where

$$R(x, y) = -\frac{|x-y|}{D^2} \coth\left(\frac{\pi|x-y|}{D}\right) \quad (59)$$

and $D > 0$ is an adjustable parameter called tension. For our purpose it seems that a reasonable choice for N is around 20.

Once the three functions have been determined, we use Eqs. (19), (20), (21c), and (22) to calculate the ionic potential $v_{ion}(r)$. Equations (22) are integrated using a finite numerical grid to find the self-consistent charge density $n(r)$ (see the Appendix). The potential $v_{HXC}(r)$ obtained from this density is fitted to a RST over $[0, r_c]$ to give $v_{ion}(r)$ in the same form. Outside the core $A(r) = B(r) = 0$ and, from Eq. (27),

$$v_{ion}(r) = -\frac{Z}{r} + v_{HXC}^{FC}(r) - v_{HXC}(r). \quad (60)$$

For large r , $v_{ion}(r)$ behaves like $-Z_v/r$ but right outside the core it may still slightly depart from this asymptotic behavior, so outside the core we found it convenient to fit it to a superposition of error functions times the Coulombic tail:

$$v_{ion}^{FIT}(r) = -\frac{Z_v}{r} \sum_i c_i \operatorname{erf}(\sqrt{\alpha_i} r), \quad r \geq r_c. \quad (61)$$

IV. RESULTS AND DISCUSSION

A. General considerations on simulated annealing

The starting point of our simulated-annealing procedure is usually the pseudo-Hamiltonian of Ref. [10], which reproduces exactly only s and p angular momentum states. The whole procedure is carried on until a minimum of the cost function is reached, for which the main requirements are satisfied within the desired accuracy: typical values for the relative errors on the DFT-LDA eigenvalues are of order 10^{-4} ; on the norms, 10^{-3} [49]. Since the secondary requirements have by construction smaller weights in the cost function (Sec. III B), they are only approximately fulfilled at the minimum where we stop. Depending on the degree of fulfillment of the secondary conditions we then decide whether to really stop and take the resulting $a(r)$, $c(r)$, and $v(r)$ as our optimal solution, or, instead, to start over. So in fact, after monitoring the cost function and finding a minimum within a

given threshold, as suggested at the end of Sec. III B, we finally also separately monitor individual contributions to the cost function, and perform some sort of fine tuning which amounts to setting acceptance thresholds to individual contributions.

The simulated-annealing run (which inevitably implies some degree of arbitrariness) is made up, as usual, of many “trial and error” cycles. This is due to the very little knowledge and the great complexity of the topography of the cost function, and to the fact that the algorithm converges to the optimal solution with unit probability only in principle, as we cannot deal with infinitely long random walks. A general prescription about the most efficient way to carry on the simulated-annealing procedure is thus impossible. There are, however, two guidelines: too short a random walk means a high probability of missing the important region of the parameter space; too sudden a lowering of the temperature T means a high probability of getting frozen into a local minimum which is unacceptable. Of course “too short” and “too sudden” are problem dependent, and we can only resort to the “trial and error” strategy. In our experience (with our particular ~ 60 -parameter cost function), if the starting point of the random walk is far enough from a local minimum, or in other words if the temperature T is not too low, even two simulated-annealing runs which originate from the same starting point in the parameter space end up in two different minima, as soon as a slightly different annealing strategy is adopted. This is of course related to the complex structure of the cost function, and would sound discouraging if the goal of the simulated annealing were to pick the exact location of the absolute minimum of the cost function. Fortunately, however, once a simulated annealing run finds a local minimum which matches our accuracy requirements, then all the (in principle different) local minima which are reached by independent simulated annealing runs originating from that starting point are of comparable accuracy. So for our purpose the strategy is perfectly adequate.

B. Some examples

A number of pseudo-Hamiltonians have been obtained by means of the powerful method of simulated annealing. In particular, for alkali metals from Li through Cs, starting from the pseudo-Hamiltonian of Ref. [10], it is possible to end up with a more transferable pseudo-Hamiltonian, as we will show in detail for Na. Another region of the periodic table that has been investigated is the second row for which, besides Na, we have built pseudo-Hamiltonians for Al, Si, P, and Cl. Among these the case of Si will be detailed in the following. The third row has also been attacked with positive results for Ge and As, while we still have difficulties for the first-row elements: we will present some results for C that are far from being satisfactory, but show that something can be done and also help clarify the reasons why first-row pseudo-Hamiltonians are intrinsically less transferable. As we have seen, theoretical reasons prevent us from reproducing transition elements with standard pseudo-

TABLE I. Numerical coefficients for Si pseudo-Hamiltonian (see Sec. III C). Numbers in square brackets denote powers of 10.

$Z = 14$	$Z_v = 4$	$N = 21$
$r_c = 1.90801447[+00]$	$D = 5.00000000[-01]$	
$a_{lo} = 1.00000000[-01]$	$c_{lo} = 1.00000000[-03]$	
$c_1 = 7.01006204[+00]$	$c_2 = -5.85550349[+00]$	$c_3 = -1.54558553[-01]$
$\alpha_1 = 2.37847912[+00]$	$\alpha_2 = 2.15978820[+00]$	$\alpha_3 = 1.04377440[+00]$
λ_i^a	λ_i^c	λ_i^v
1.57773662[+00]	7.17813275[-01]	-1.22586351[+00]
-8.85236760[-01]	2.16485127[+02]	4.80429388[-02]
1.80143777[+00]	-4.97923120[+02]	-7.73525376[-01]
-1.72675285[+00]	6.83268691[+02]	3.82821268[+00]
1.75841796[+00]	-9.63053012[+02]	-9.73799267[+00]
-2.80132889[+00]	1.32586946[+03]	1.83722202[+01]
3.69441735[+00]	-1.77981302[+03]	-2.74939378[+01]
-5.16169983[+00]	2.32586387[+03]	4.00928597[+01]
7.34859550[+00]	-2.93498646[+03]	-5.54510496[+01]
-8.97216383[+00]	3.53117054[+03]	7.31762428[+01]
1.17584506[+01]	-3.98046094[+03]	-9.75429253[+01]
-1.54935995[+01]	4.16770026[+03]	1.27989123[+02]
2.03687067[+01]	-4.11444787[+03]	-1.65142887[+02]
-2.67627715[+01]	3.91064877[+03]	2.12550896[+02]
3.36901960[+01]	-3.57796012[+03]	-2.70134840[+02]
-4.14709224[+01]	3.10003116[+03]	3.35502611[+02]
5.15386069[+01]	-2.52395610[+03]	-4.06201324[+02]
-6.16352611[+01]	1.93796994[+03]	4.65263656[+02]
7.21171341[+01]	-1.40818063[+03]	-4.94131168[+02]
-8.07012089[+01]	9.67736199[+02]	4.81713922[+02]
8.62369408[+01]	-6.57305731[+02]	-4.46214160[+02]
-4.47019581[+01]	2.71342986[+02]	2.14286023[+02]
2.33283412[+00]	-1.15903468[+01]	-1.01743412[+01]
-4.45098506[-02]	9.75030914[+00]	

Hamiltonians [that is, obeying properties (P1) to (P4)] and we have not considered them. Other regions, such as the second column of the periodic table, are instead not expected to be problematic and will be investigated in the near future.

The numerical coefficients through which the generated Si pseudo-Hamiltonian is expressed, Eq. (50) and Sec. III C, are listed in Table I. For each pseudo-Hamiltonian obtained from the simulated-annealing procedure a DFT-LDA atomic calculation has been performed. This has been done in order to check the numerical errors on the eigenvalues of the reference configuration with respect to the corresponding full-core atoms, since they are only estimated and never exactly calculated

(see the Appendix) during the simulated-annealing run. The reference configuration chosen for Si is $s^{0.8}p^{2.4}d^{0.2}$ ($\ell = 0, 1, 2$) with core radius $r_c = 1.91$ a.u., for Na $s^{0.6}p^{0.1}$ ($\ell = 0, 1$) with $r_c = 2.40$ a.u., and for C it is the ground state s^2p^2 ($\ell = 0, 1$) with $r_c = 1.31$ a.u. Tables II, III, and IV show the results for Si, Na, and C compared with full-core and standard nonlocal pseudopotential [33] calculations; we also consider other relevant valence configurations, such as the ground state. The functions $A(r)$, $B(r)$, and $v_{ion}(r)$, together with the corresponding radial wave functions $\chi_\ell(r)$ for the reference configuration, are shown in Fig. 1 for Si and Fig. 2 for Na. The full-core wave functions are shown for comparison: we notice that neither the error on the eigenvalue nor the error on the

TABLE II. Atomic energies in atomic units for Si in the reference configuration $s^{0.8}p^{2.4}d^{0.2}$ and in the ground state s^2p^2 . The eigenvalues ϵ_ℓ and the total energies E are shown for the pseudo-Hamiltonian, the full-core atom, and the nonlocal pseudopotentials of Ref. [33].

	Configuration	ϵ_s	ϵ_p	ϵ_d	E
PH	$s^{0.8}p^{2.4}d^{0.2}$	-0.62778	-0.35861	-0.07714	-3.24934
	s^2p^2	-0.39899	-0.15268		-3.76002
Full core	$s^{0.8}p^{2.4}d^{0.2}$	-0.62788	-0.35866	-0.07714	-288.25400
	s^2p^2	-0.39989	-0.15322		-288.76510
Nonlocal	$s^{0.8}p^{2.4}d^{0.2}$	-0.62588	-0.35752	-0.07816	-3.24021
	s^2p^2	-0.39990	-0.15327		-3.75042

TABLE III. Atomic energies in atomic units for Na in the reference configuration $s^{0.6}p^{0.1}d^0$ and in the ground state s^1 . The eigenvalues ϵ_ℓ and the total energies E are shown for the pseudo-Hamiltonian, the full-core atom, and the nonlocal pseudopotentials of Ref. [33] (see text).

	Configuration	ϵ_s	ϵ_p	ϵ_d	E
PH	$s^{0.6}p^{0.1}d^0$	-0.15928	-0.07313	-0.01218	-0.13843
	s^1p^0	-0.10466	-0.02824		-0.18617
Full core	$s^{0.6}p^{0.1}d^0$	-0.15931	-0.07314	-0.01271	-161.56832
	s^1p^0	-0.10371	-0.02847		-161.61580
Nonlocal	$s^{0.6}p^{0.1}d^0$	-0.15724	-0.07738	-0.01259	-0.13767
	s^1p^0	-0.10357	-0.03205		-0.18437

norm can be resolved by eye; in other words, the tails of the functions are perfectly overlapping. This results from numerical optimization (not from numerical inversion as in the Hamann-Schlüter-Chiang method of Ref. [9] and related ones) and is thus a remarkable success of the procedure presented here. Even in the case of Na we monitor the d eigenvalue and eigenvector (with zero occupation in the reference configuration $s^{0.6}p^{0.1}d^0$), although for this element we did not include the d wave in the construction of the pseudo-Hamiltonian; for the d wave we find (Table III) $\epsilon_d \geq \epsilon_d^{FC}$, as it must be (see the end of Sec. IID); the eigenvalue ϵ_d is even very close to the full-core eigenvalue (only a few percent off ϵ_d^{FC}), but we see from Fig. 2(d) that the norm conservation of $\chi_d(r)$ is, instead, not as good: the tails of the wave functions do not overlap. This shows that unless all three spd waves are explicitly optimized the resulting pseudo-Hamiltonian is inevitably poorer.

C. The transferability problem

To put to test the pseudo-Hamiltonian against the true, full-core ion, we have performed a number of atomic calculations. Let us first examine our plots of logarithmic derivatives, versus energy, shown below in Fig. 3 for C, Fig. 4 for Na, and Fig. 5 for Si. The logarithmic derivatives are always taken at the covalent radius; in the figures we show $R'_\ell(\epsilon, r)/R_\ell(\epsilon, r)$ rather than $x_\ell(\epsilon, r)$ as given in Eq. (29); they are related by

$$R_\ell(\epsilon, r) = \frac{\chi_\ell(\epsilon, r)}{r}, \quad (62)$$

$$\frac{R'_\ell(\epsilon, r)}{R_\ell(\epsilon, r)} = r x_\ell(\epsilon, r) - 1. \quad (63)$$

The case of carbon illustrates an important difference be-

tween pseudo-Hamiltonians and nonlocal pseudopotentials. Figure 3 shows the s -wave logarithmic derivatives [(a) and (c), left panels] and the p -wave logarithmic derivatives [(b) and (d), right panels] as a function of energy for two different carbon pseudo-Hamiltonians (shown in Fig. 6). Three logarithmic-derivative curves are shown in each panel: the full-core (solid) and the nonlocal pseudopotential (short-dashed), which are always so close to each other as to appear almost indistinguishable, and the pseudo-Hamiltonian (dashed), which instead, sooner or later, departs from the full-core and nonlocal pseudopotential curves. The upper panels refer to a carbon pseudo-Hamiltonian [Fig. 6(a)] which exactly corresponds to a nonlocal pseudopotential for carbon [50] (used as a benchmark throughout the figure); to be precise, in the reference state, the upper-panel pseudo-Hamiltonian has identical s and p wave functions as the benchmark nonlocal pseudopotential. As expected from Eqs. (28) and (30), at the reference energy (shown as a bullet), the logarithmic derivative and its first energy derivative are identical for all curves. It is also apparent that higher energy derivatives must be different for pseudo-Hamiltonian and nonlocal pseudopotential, because the two curves, at some point, evidently depart from each other. This can be understood by comparing the Eqs. (31) and (32) at the end of Sec. IIC, which deal with the “extended norm conservation” for nonlocal pseudopotentials [29] and pseudo-Hamiltonians [30]. The upper panels of Fig. 3 show that, for carbon, this effect is large; that the effect is physically relevant can be seen by independent atomic calculations (not presented here), which show that the upper-panel pseudo-Hamiltonian, whose ground-state wave functions are identical to the well-transferable nonlocal pseudopotential carbon, is in fact much less transferable [31]. To obtain a more transferable pseudo-Hamiltonian [Fig. 6(b)] one can for example, for each ℓ , impose the agreement of full-core and

TABLE IV. Atomic energies in atomic units for C in the reference state s^2p^2 that is also the ground state. The eigenvalues ϵ_ℓ and the total energies E are shown for the pseudo-Hamiltonian, the full-core atom, and the nonlocal pseudopotentials of Ref. [33].

	Configuration	ϵ_s	ϵ_p	ϵ_d	E
PH	s^2p^2	-0.50128	-0.19931		-5.34973
Full core	s^2p^2	-0.50120	-0.19925		-37.42832
Nonlocal	s^2p^2	-0.50139	-0.19857		-5.34505

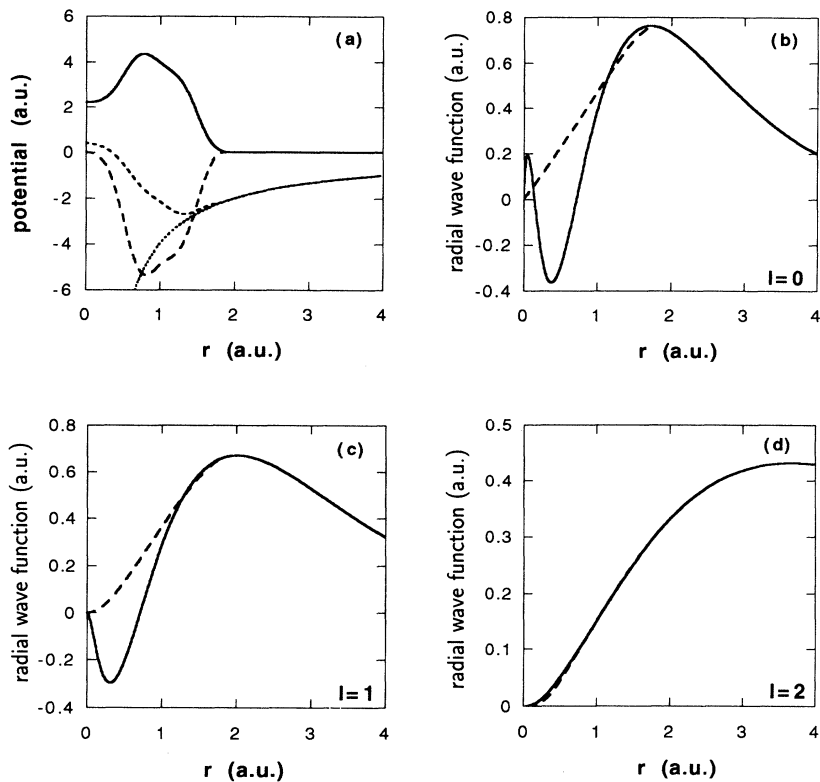


FIG. 1. Pseudo-Hamiltonian for Si: the reference configuration is $s^{0.8}p^{2.4}d^{0.2}$ and the core radius $r_c = 1.91$ a.u. (a) Functions $A(r)$ (solid line), $B(r)$ (long-dashed), and $v_{ion}(r)$ (short-dashed), and Coulomb potential $-Z_v/r$ (dotted). (b) s wave function, (c) p wave function, and (d) d wave function for the full-core atom (solid line) and the pseudo-Hamiltonian (dashed) in the reference configuration.

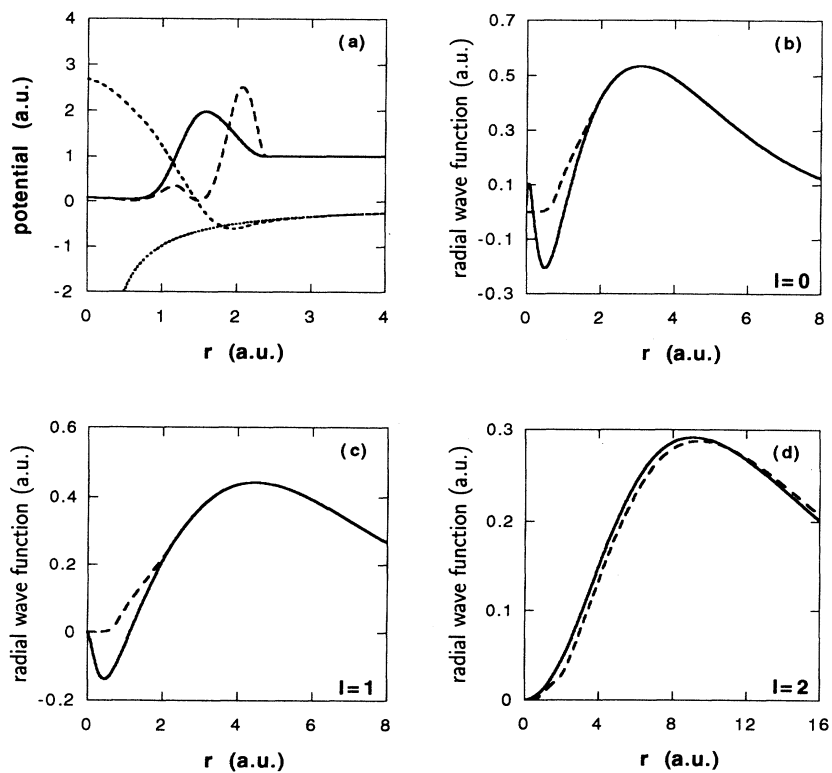


FIG. 2. Pseudo-Hamiltonian for Na: the reference configuration is $s^{0.8}p^{0.1}$ and the core radius $r_c = 2.40$ a.u. (a) Functions $A(r)$ (solid line), $B(r)$ (long-dashed), and $v_{ion}(r)$ (short-dashed), and Coulomb potential $-Z_v/r$ (dotted). (b) s wave function, (c) p wave function, and (d) d wave function for the full-core atom (solid line) and the pseudo-Hamiltonian (dashed) in configuration $s^{0.6}p^{0.1}d^0$ (see text).

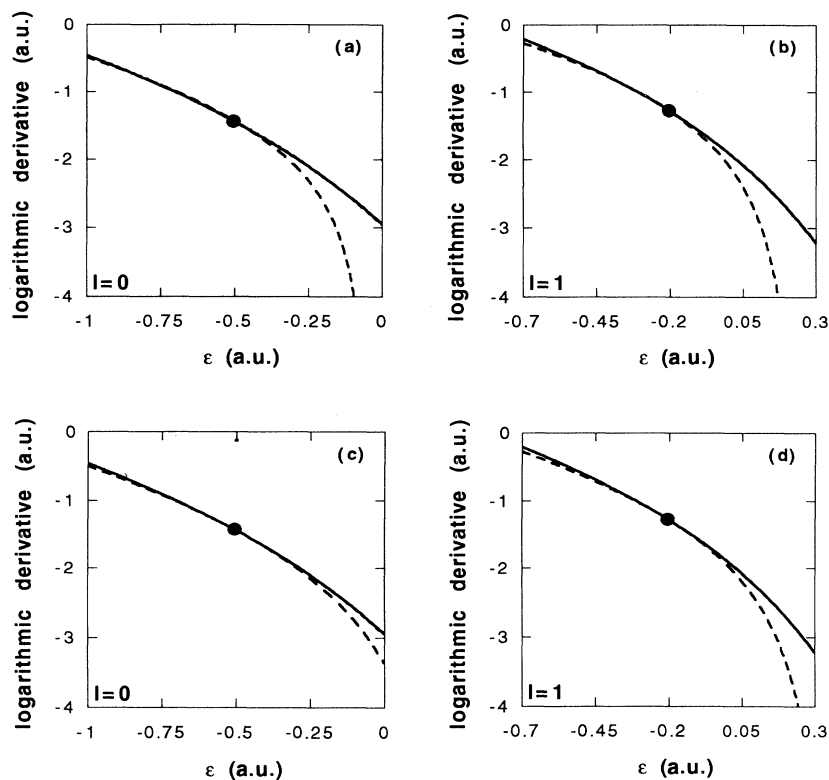


FIG. 3. Logarithmic derivatives for C: (a) s -wave and (b) p -wave logarithmic derivative versus energy for the full-core atom (solid line), the pseudo-Hamiltonian described in text (dashed), and the corresponding nonlocal pseudopotentials (short-dashed) in the ground state s^2p^2 (see text). (c) s -wave and (d) p -wave logarithmic derivative versus energy for the full-core atom (solid line), a different pseudo-Hamiltonian built as described in text (dashed), and the same nonlocal pseudopotentials as above (short-dashed) in the ground state s^2p^2 . Nonlocal pseudopotential and full-core curves are almost perfectly overlapping. See also text.

pseudologarithmic derivatives at two different reference energies rather than just one. Such an additional constraint was mentioned as a possibility in Sec. III A, and has been implemented for carbon. The results are shown in the bottom panels of Fig. 3. We see that, after imposing this additional constraint, the logarithmic derivatives of the pseudo-Hamiltonian follow the good ones over a wider energy interval; independent self-consistent atomic tests suggest that the pseudo-Hamiltonian transferability has improved considerably. Yet the transferability of the pseudo-Hamiltonian remains for carbon (as well as other first-row atoms) less satisfactory than that of nonlocal pseudopotentials. Why are first-row atoms more difficult for the pseudo-Hamiltonian method? The likely reason for that is the following. To have good higher order energy derivatives of the logarithmic derivative one needs, in the pseudo-Hamiltonian case, the agreement of integrals involving both the valence radial wave function and the function $a(r)$ [Eq. (32)]. But in the first-row atoms there is very little freedom for the p radial pseudo-wavefunction, which cannot depart much from the original full-core p wave function: besides having the same behavior in the origin, the same norm inside the core radius, and the same value and derivative at the core radius, *they both have no nodes*. As a result, two opposite situations are found for first-row pseudo-Hamiltonians and nonlocal pseudopotentials: for nonlocal pseudopotentials the p -wave logarithmic derivatives are almost automatically very good [all higher order energy derivatives give almost identical integrals for full-core and nonlocal pseudopotentials in Eq. (31)], while for pseudo-Hamiltonians the same

physics (little freedom left for first-row p pseudo-wavefunctions inside the core), combined with the presence of a sizable $a(r)$ in all the relevant integrals of Eq. (32), yields—even when effort is taken to improve the energy dependence, as done in the bottom panels of Fig. 3—poorer logarithmic derivatives.

Similar logarithmic-derivative plots have been obtained for Na and Si. They belong to the second row, so the problem just discussed for carbon (and first-row atoms in general), which is of course related to their stronger nonlocality, is much less pronounced; as shown in Figs. 4 and 5 much more transferable pseudo-Hamiltonians can be obtained. In these two figures the s -, p -, and d -wave logarithmic derivatives are shown as a function of energy. The solid, short-dashed, and dashed lines correspond to the full-core atom, the nonlocal pseudopotentials, and the pseudo-Hamiltonian, respectively; here we are using standard nonlocal pseudopotentials [33]. For the construction of the Na pseudo-Hamiltonian (Fig. 4) no attempt was made to optimize the d wave [the $\ell = 2$ quantities were not included in the cost function Eq. (55)]; the corresponding logarithmic derivative is evidently less good, but still acceptable, also because the d states are high up in energy and are not expected to play an important role in the chemistry and physics of this ion. The s logarithmic derivative is, instead, excellent, and the p is even better than the nonlocal pseudopotential. The case of Si, finally, is a good introduction to the next set of atomic tests, not based on logarithmic derivatives. From the logarithmic-derivative plots (Fig. 5) the nonlocal pseudopotential would appear

slightly more transferable than the pseudo-Hamiltonian (the nonlocal pseudopotential tracks the full-core atom slightly more closely), but crystalline calculations, as well as other self-consistent tests, suggest that the transfer-

ability of the pseudo-Hamiltonian obtained for Si is, instead, slightly better than standard nonlocal pseudopotentials. These differences in the ionic transferability are at a much finer level of accuracy than just seen for carbon, but are a good way to emphasize an as-

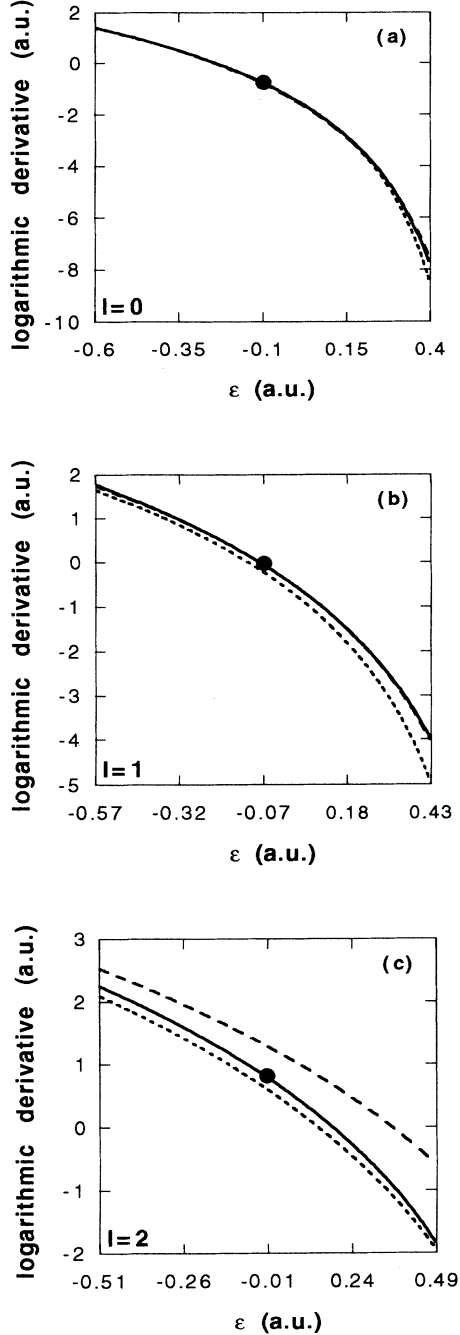


FIG. 4. Logarithmic derivatives for Na: (a) s -wave and (b) p -wave logarithmic derivative versus energy for the full-core atom (solid line), the pseudo-Hamiltonian (dashed), and nonlocal pseudopotentials of Ref. [33] (short-dashed) in the ground state s^1 ; (c) d -wave logarithmic derivative as above but for configuration $s^{0.6}p^{0.1}d^0$. s and p logarithmic derivatives for the full-core atom and the pseudo-Hamiltonian are almost indistinguishable. See also text.

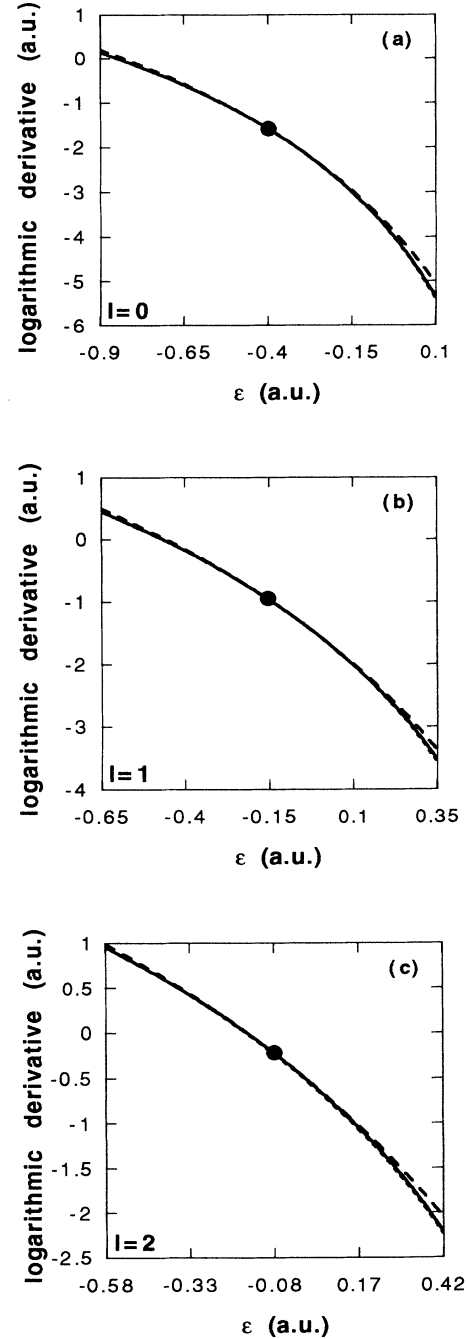


FIG. 5. Logarithmic derivatives for Si: (a) s -wave and (b) p -wave logarithmic derivative versus energy for the full-core atom (solid line), the pseudo-Hamiltonian (dashed), and nonlocal pseudopotentials of Ref. [33] (short-dashed) in the ground state s^2p^2 ; (c) d -wave logarithmic derivative as above but for the reference configuration. Nonlocal pseudopotential and full-core plots are perfectly overlapping. See also text.

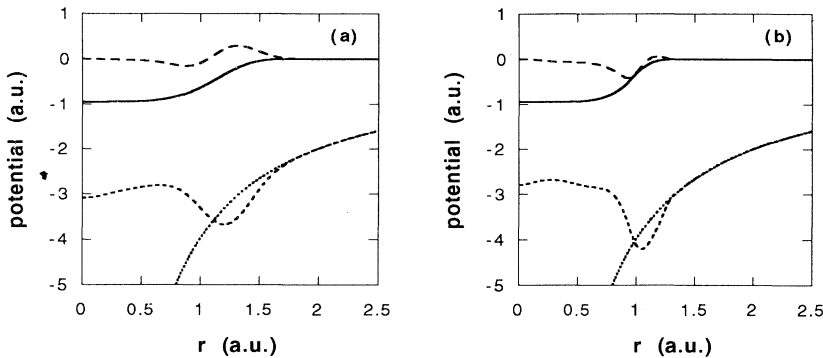


FIG. 6. Pseudo-Hamiltonians for C: the reference configuration is s^2p^2 . $A(r)$, $B(r)$, $v_{ion}(r)$ and Coulomb potential $-Z_0/r$ as in Fig. 2. (a) Bachelet-Ceperley-Chiocchetti-like pseudo-Hamiltonian [51]. (b) Improved logarithmic-derivative pseudo-Hamiltonian. See also text.

pect of pseudopotential theory empirically known to specialists, but only recently clarified and rationalized by Teter [17], namely, that the agreement between full-core and pseudologarithmic derivatives gives only partial information on ionic transferability. Let us briefly recall why. To obtain logarithmic-derivative plots, the electronic charge density is frozen into some fixed valence configuration (thus the screening potential v_{HXC} is also fixed), and then the solution of the radial Schrödinger equation [Eqs. (17), (22), and (33)] is obtained at many different energies. The energy is varied, but the charge density remains fixed. Such an energy sweep, thus, only partially mimics the changed boundary conditions experienced by the wave functions when the atom is put into a molecular or solid-state environment: a faithful energy dependence implies a good ionic transferability only when the total amount of valence charge density contained inside the core radius is very small [16,33], and the core and valence charge densities do not overlap significantly [51]. The more accurately these two conditions are met, the less important are the effects of the self-consistent rearrangement of the charge density inside the core, and the more reliable are the logarithmic-derivative plots as transferability tests. If, instead, these two conditions are not met, then alternative tests which do involve self-consistency are more conclusive. We present some of them here. In comparison to the “chemical hardness” test proposed by Teter [17], which has the advantage of addressing nonspherical charge perturbations, ours are, unlike his, extended to finite charge distortions. Three distinct types of tests involving self-consistency have been performed: a change of the atomic boundary conditions, a change of the orbital occupation (presented in this subsection), and a set of crystal calculations (presented in the next subsection). We have put to test the pseudo-Hamiltonian single-particle eigenvalues ϵ_ℓ^{PH} and ϵ_ℓ^{FC} and the excitation energies $E^{PH} - E_{gs}^{PH}$ and $E^{FC} - E_{gs}^{FC}$ (i.e., the total-energy differences between excited states and ground states of isolated atoms) against the corresponding full-core counterparts. For completeness, we have also included in our comparison standard nonlocal pseudopotentials [33] (index PP in the calculated quantities), as they have been widely and successfully used, and represent an obvious quality reference. Before discussing the atomic tests, we note that the appropriate comparison is between full-core and valence-only systems within an identical (approximate) DFT-LDA framework. Most im-

portant is to note that, as pseudopotential methods rely on the frozen-core approximation [52], benchmark full-core calculations should also keep the core frozen into a specified reference configuration. While the results presented in this subsection do not substantially change if we replace the relaxed-core with the frozen-core calculations, we will see in the next subsection that this difference can be relevant in some situations. Experimental quantities are quoted where relevant only for completeness. We now come to a discussion of the transferability tests.

In the first group of tests we have evaluated the change of pseudoeigenvalues and total excitation energies with respect to the corresponding full-core quantities, while changing the boundary conditions for the atomic wave functions. The atomic orbitals were confined within a sphere of radius R , or, in other words, the position R of the radial nodal surface, defined by the equation

$$\chi_\ell(R) = 0 \quad \forall \ell, \quad (64)$$

was moved from $R = +\infty$ (isolated atom) towards smaller and smaller radii, covering a wide range of spherical boundary conditions, which to some extent could mimic the transition from the isolated atom to more closely packed environments [30]. In this group of tests the orbital occupation is always that of the ground state, so that, for the atoms under consideration, only the angular momenta $\ell = 0, 1$ are involved; Fig. 7 shows the results for Si [upper panels (a) and (b)] and Na [lower panels (c) and (d)]. The left panels of Fig. 7 [(a) and (c)] deal with single-particle eigenvalues. They show $\Delta\epsilon_\ell^{PH} = \epsilon_\ell^{PH} - \epsilon_\ell^{FC}$ ($\Delta\epsilon_s^{PH}$ solid line, $\Delta\epsilon_p^{PH}$ long-dashed) and $\Delta\epsilon_\ell^{PP} = \epsilon_\ell^{PP} - \epsilon_\ell^{FC}$ ($\Delta\epsilon_s^{PP}$ short-dashed, $\Delta\epsilon_p^{PP}$ dotted), as a function of R^{-1} . In Fig. 7(a) the s and p curves for the Si pseudo-Hamiltonian are slightly flatter than the corresponding curves for nonlocal pseudopotentials. This means that, as the radial node moves inward, the pseudo-Hamiltonian eigenvalues track the corresponding full-core eigenenergies slightly more closely than nonlocal pseudopotentials, i.e., the opposite of what the analysis of the logarithmic derivatives alone would have suggested [53]. In Fig. 7(c) the p curve for the Na pseudo-Hamiltonian is much closer to that for nonlocal pseudopotentials, this time in agreement with the expectations suggested by the logarithmic-derivative plot of Fig. 5(b). The behavior is the opposite for the s curves (but on a finer level), once more in

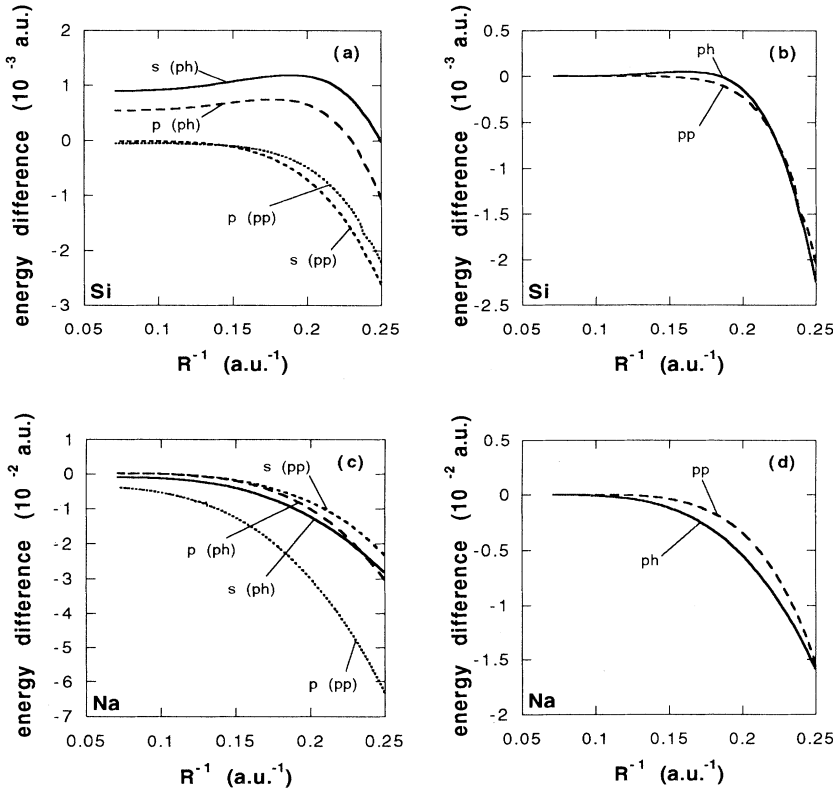


FIG. 7. As a function of the inverse distance of the radial nodal surface from the nucleus (R^{-1}) are shown (a) Si s and p eigenvalue differences, pseudo-Hamiltonian and nonlocal pseudopotentials of Ref. [33] minus full-core, $\Delta\epsilon^{PH} = \epsilon^{PH} - \epsilon^{FC}$ ($\Delta\epsilon_s^{PH}$: solid line, $\Delta\epsilon_p^{PH}$: long-dashed) and $\Delta\epsilon^{PP} = \epsilon^{PP} - \epsilon^{FC}$ ($\Delta\epsilon_s^{PP}$: short-dashed, $\Delta\epsilon_p^{PP}$: dotted); (b) Si excitation energy differences, pseudo-Hamiltonian and nonlocal pseudopotentials of Ref. [33] minus full-core, $\Delta E^{PH} = (E^{PH} - E_{gs}^{PH}) - (E^{FC} - E_{gs}^{FC})$ (solid line) and $\Delta E^{PP} = (E^{PP} - E_{gs}^{PP}) - (E^{FC} - E_{gs}^{FC})$ (long-dashed); (c) and (d) the same quantities for Na. s and p labels, respectively, refer to $\ell = 0$ and $\ell = 1$, ph and pp to pseudo-Hamiltonian and nonlocal pseudopotentials. See also text.

contrast with the behavior of logarithmic derivatives in Fig. 5(a), where the pseudo-Hamiltonian curve is closer to the full-core one. The right panels of Fig. 7 [(b) and (d)] deal with total-energy differences: they show $\Delta E^{PH} = (E^{PH} - E_{gs}^{PH}) - (E^{FC} - E_{gs}^{FC})$ (solid line) and $\Delta E^{PP} = (E^{PP} - E_{gs}^{PP}) - (E^{FC} - E_{gs}^{FC})$ (dashed), as a function of R^{-1} , for both Si and Na. Here the difference between pseudo-Hamiltonian and nonlocal pseudopotentials is less pronounced. For both pseudoions the curve is very similar, and can be easily understood in terms of differences between the full-core and the valence-only atom; these differences are, in fact, almost independent of the pseudionization scheme. When the atomic charge density is confined within a sphere of smaller and smaller radius R , core and valence begin to overlap significantly, and the LDA exchange-correlation functional will be affected by the absence of the core charge in the pseudo case. This effect would be obviously greatly reduced by the nonlinear core correction of Louie, Froyen, and Cohen [51], but, on the other hand, the introduction of such a density-dependent correction would unfortunately make our pseudo-Hamiltonian useless for quantum Monte Carlo calculations [54].

In the second kind of group of tests we have studied the response of the pseudo-Hamiltonian and nonlocal pseudopotentials to a change in the orbital occupation (see the Appendix), compared to the corresponding response of the full-core atom [49]. Single-particle and total energies are defined as above, and the orbital occupation has been varied in two different ways: in one case the total electronic charge was kept constant and equal to

its ground state value, i.e., the valence charge was just moved from one orbital to another (Fig. 8), in the other case the total valence charge was allowed to vary, and it was decreased from the ground state to the doubly ionized Si atom, or to the simply ionized Na atom (Fig. 9). More precisely, in Figs. 8(a) and 8(b), the occupation of the s and p orbitals of Si has been varied from s^2p^2 (ground state) to s^0p^4 : the curves corresponding to the pseudo-Hamiltonian are flatter than the curves of nonlocal pseudopotentials. This means that, once again, the pseudo-Hamiltonian more closely follows the full-core response than nonlocal pseudopotentials. The lower panels of Fig. 8 [(c) and (d)] show, for Na, the same behavior just described for Si (but now the occupation goes from s^1p^0 to s^0p^1), and the discrepancy between pseudo-Hamiltonian and nonlocal pseudopotentials is even more marked. In the ‘‘ionization test’’ (Fig. 9), the occupation for the s orbital of Si is kept fixed and equal to s^2 , while the p occupation ranges from p^0 (ion Si^{2-}) to p^2 [upper panels (a) and (b)]; for Na, only the occupation of the s orbital is varied from s^0 to s^1 , with the p orbital unoccupied [Figs. 9(c) and 9(d)]. For both Si and Na, the response of the eigenvalues of the pseudo-Hamiltonian is closer to the full-core behavior than for nonlocal pseudopotentials [Fig. 9, panels (a) and (c)]; in the case of total energies the situation is the same for Na [Fig. 9(d)] but reversed for Si [Fig. 9(b)], with the nonlocal pseudopotential curve more closely tracking the full-core atom in the latter case. This shows that the transferability at a really fine level of accuracy is a subtle game: for Na, where the overall transferability is less

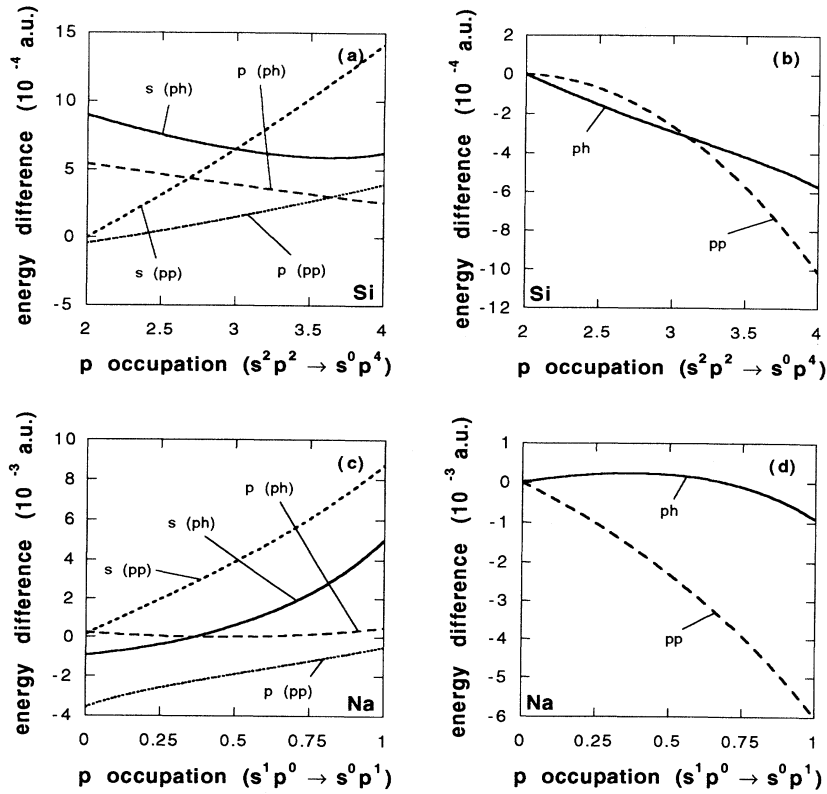


FIG. 8. As a function of Kohn-Sham p occupation number are plotted (a) $\Delta\epsilon^{PH}$ ($\Delta\epsilon_s^{PH}$: solid line, $\Delta\epsilon_p^{PH}$: long-dashed) and $\Delta\epsilon^{PP}$ ($\Delta\epsilon_s^{PP}$: short-dashed, $\Delta\epsilon_p^{PP}$: dotted); (b) ΔE^{PH} (solid line) and ΔE^{PP} (long-dashed) for Si while changing the configuration from $s^2 p^2$ to $s^0 p^4$; (c) and (d) the same quantities for Na while changing the configuration from $s^1 p^0$ to $s^0 p^1$. The labels are the same as in Fig. 7. See also text.

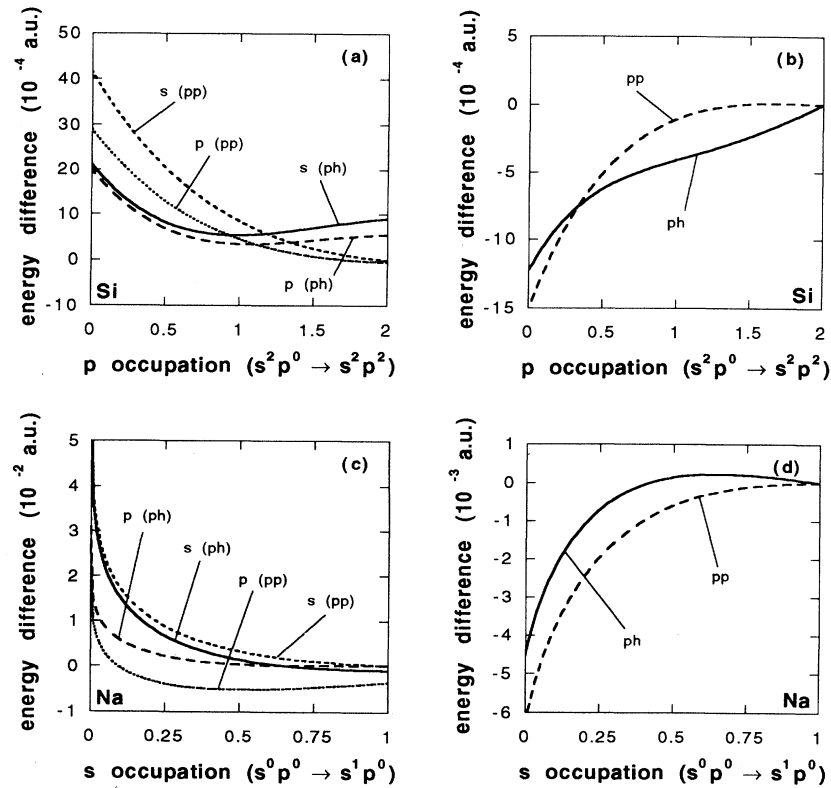


FIG. 9. (a) $\Delta\epsilon^{PH}$ ($\Delta\epsilon_s^{PH}$: solid line, $\Delta\epsilon_p^{PH}$: long-dashed) and $\Delta\epsilon^{PP}$ ($\Delta\epsilon_s^{PP}$: short-dashed, $\Delta\epsilon_p^{PP}$: dotted) and (b) ΔE^{PH} (solid line) and ΔE^{PP} (long-dashed) are plotted as a function of Kohn-Sham p occupation number for Si, while changing the configuration from $s^2 p^0$ to $s^2 p^2$. (c) and (d) are the same quantities for Na plotted as a function of Kohn-Sham s occupation number while changing the configuration from $s^0 p^0$ to $s^1 p^0$. The labels are the same as in Fig. 7. See also text.

good, logarithmic-derivative and eigenvalue plots give a coherent picture, while for Si, where the overall transferability is excellent, the tests give contradictory results and thus the slight quality differences cannot be conclusively deduced from logarithmic-derivative plots. Notice, however, that both in the previous test and in this one the energy scale on which the performance of different silicon pseudoatoms (nonlocal pseudopotentials vs pseudo-Hamiltonian) may differ is so small that questions may legitimately arise about which one of the various transferability tests should be taken as the most meaningful measure of this property. So crystal or molecular calculations are not expected to add much to the picture already gained by atomic tests (as far as transferability is concerned) in the case of sodium, while, in the case of silicon, they may represent the only way to resolve a puzzle. This transferability puzzle is by no means an idle question, since it is precisely on this energy scale that recent variational Monte Carlo and quantum Monte Carlo calculations based on nonlocal pseudopotentials and pseudo-Hamiltonians, respectively, disagreed [4,13].

D. Crystal properties

To substantiate our previous statement with numbers, before concluding our work, we proceed to the calculation of the bulk properties of crystalline silicon and sodium. The environments experienced by an isolated atom and an atom in the crystal are different, and such a difference just amounts to the kind of transferability one is interested in; this calculation enables an independent and direct inspection of the quality of the pseudo-Hamiltonian being studied, which complements the tests discussed previously (especially as far as nonspherical terms are concerned). A good transferability of the pseudo-Hamiltonian within the DFT-LDA also appears as a prerequisite for reliable further use in a QMC simulation.

We have studied insulating Si in the diamond structure and metallic Na in the bcc structure, at zero temperature, by means of DFT-LDA total-energy calculations. A suitably modified plane-wave LDA total-energy code was used for the pseudo-Hamiltonian and nonlocal pseudopotentials calculations of the valence-only crystal [7], while the full-core crystal was studied by means of the all-electron full-potential linear-muffin-tin-orbitals (LMTO) method [55]. The full-core crystal calculation was performed both relaxing self-consistently all the electronic states and freezing the core states in the atomic ground-state configuration. In the latter case, the core density

to be used in the electrostatic and exchange-correlation terms was obtained by overlapping the free-atom cores at each iteration, while the one-particle core eigenvalues were added to the total energy (for details see Ref. [56]).

Some technical points are worth mentioning. As can be guessed from Figs. 1 and 2, the pseudo-Hamiltonian may require a rather high energy cutoff in a plane-wave calculation. Converged quantities were obtained for cutoff energy of 50 Ry for Si, while Na required 25 Ry. The setup of Hamiltonian matrices is 3–5 times faster than with conventional nonseparable nonlocal pseudopotentials for the matrix sizes of up to 1500 used here. On the other hand, the kinetic operators of the pseudo-Hamiltonian cause the kinetic energy to be nondiagonal in Fourier space, so that the energy cutoff should be increased gradually during the self-consistent cycle; the convergence of the latter is delayed somewhat. In the full-core calculations, the crystal was represented by well-packed non-overlapping atom-centered spheres, the muffin-tin radius being 98% of that of touching spheres. As is usually done within LMTO methods [57], we insert empty spheres, of the same radius as the atomic spheres, in the interstitial regions of the diamond structure. The basis we used consisted of three Hankel functions with decay energies -0.7 , -1.0 , and -2.3 Ry, augmented for $\ell \leq 2$, which corresponds to 27 LMTO's per atom. For both Si and Na we included in the valence $3s$, $3p$, and $3d$ states; for Na, the $2p$ states were treated as delocalized semicore states.

The Brillouin zone summation for Si was done on the standard 10-point mesh [58]. Its treatment in metallic Na is instead worth some comments. In metals, to accelerate the convergence of the summation in the presence of a Fermi surface, an artificial broadening is often imposed on the energy distribution of electronic states. This is equivalent to assigning a fictitious nonzero temperature to the electron gas. The smoothing of the step distribution function can be enforced, e.g., by adopting a $T \neq 0$ Fermi-Dirac distribution, or approximating the δ function by a Gaussian of width $\Delta = T$ (the two procedures are not equivalent). The problem is that the exact result is recovered only in the limit $\Delta \rightarrow 0$, and reaching this limit requires again a very large (in principle infinite) number of k points. An operative solution is given by the procedure of Gillan [59], who gave a prescription for a “generalized free energy” which deviates from the $\Delta = 0$ value for the total energy by terms of $O(\Delta^3)$. De Vita [60] has recently generalized this approach to arbitrary broadening schemes, indicating that the deviation might even be $O(\Delta^4)$: indeed his treatment is equivalent in principle to the first-order Methfessel-Paxton formula [61], as our results confirm for

TABLE V. Comparison between lattice constants and cohesive energies for the Na pseudo-Hamiltonian calculated with the methods of Needs, Martin, and Nielsen [62], Fu and Ho [63], and Gillan and De Vita [59,60].

	Lattice constant (Å)	Cohesive energy (eV/atom)
Needs-Martin-Nielsen	4.07	0.61
Fu-Ho	4.36	1.10
Gillan-De Vita	4.19	0.86

TABLE VI. Bulk properties of Si crystal (see text). Experimental data are from Ref. [64]. FLAPW indicates the full-potential linearized augmented-plane-wave method.

	Lattice constant (\AA)	Cohesive energy (eV/atom)	Bulk modulus (kbar)
PH (this work)	5.44	5.04	912
PH (Ref. [10])	5.46	5.08	916
Nonlocal	5.37	5.31	968
Full core (frozen core)	5.42	5.04	960
Full core (relaxed core)	5.41	5.25	958
Full core (relaxed core, FLAPW [65])	5.41	5.28	960
Full core (relaxed core, FLAPW [66])	5.43	5.24	998
Expt.	5.43	4.63	992

the present system. We adopted a Gaussian broadening of 0.075 Ry, and find 44 k points [58] to be sufficient to give converged results. We warn that, evaluating the total energy at finite Δ with the techniques suggested by Needs, Martin, and Nielsen [62] and Fu and Ho [63], one can run into severe problems, as far as cohesive energy and equilibrium lattice constant are concerned. These problems are clearly illustrated by our Table V, where the different broadening schemes are compared for the sodium crystal; here the electron-ion interaction is always represented by the pseudo-Hamiltonian. Based on Table V we choose the Gillan-De Vita scheme for all the following sodium crystals. Comparisons of pseudo-Hamiltonians, pseudopotentials, and full-core atoms are instead shown in Tables VI and VII. Corrections for zero-point motions are not included. The performance of the pseudo-Hamiltonian for Si as compared to the full-core results is remarkably good; in particular, we observe that the frozen full-core cohesive energy is very well reproduced. For Na, the structural properties of the pseudo-Hamiltonian crystal are excellent but the absolute cohesive energy is underestimated with respect to the all-electron result. The satisfactory results are all the more remarkable considering the difficulties normally encountered by pseudopotentials in treating alkali elements. Both Si and Na have a slightly larger lattice constant and a smaller bulk modulus when the core is frozen into its free-atom shape, an effect discussed in greater detail in Ref. [56].

V. CONCLUSIONS

Accurate pseudo-Hamiltonians, which are useful and conceptually simple tools for the quantum Monte Carlo simulations of many valence-only systems, are much more difficult to construct than nonlocal pseudopotentials; it is precisely their (very desirable) local character which,

because of complicated related constraints, makes any simple Hamann-Schlüter-Chiang-like construction, based on straight numerical inversion, essentially inapplicable. Moreover, unlike nonlocal pseudopotentials, local pseudo-Hamiltonians cannot even in principle deal with transition-metal ions, and encounter considerable practical difficulties also with the (strongly nonlocal) first-row elements. In this paper, besides giving a detailed account of the pseudo-Hamiltonian method, we propose a numerical technique based on simulated-annealing cycles, and show that it is capable of yielding accurate pseudo-Hamiltonians for that portion of the periodic table of the elements where they really work well (the simple sp -bonded atoms). For first-row elements and transition elements conceptually less simple approaches are needed [5], but for those chemical elements for which it works well the pseudo-Hamiltonian represents a clean and accurate tool.

As far as transferability is concerned, our extensive atomic and solid-state tests suggest that the quality of our pseudo-Hamiltonians is comparable to standard nonlocal pseudopotentials. A surprise of our crystal tests was that the cohesive energy of a relaxed-core silicon crystal is larger (in the local-density approximation) by as much as 0.2 eV/atom than the frozen-core silicon crystal. This simple finding was never previously presented in the literature, at least to our knowledge, and suggests some caution when comparing on this energy scale cohesive energies from various quantum Monte Carlo valence-only simulations and experimental values [4,13]. This finding also shows that, as far as cohesive energies are concerned, the Si pseudo-Hamiltonians are, on the 0.2 eV/atom scale, slightly more transferable (and not less transferable) than standard pseudopotentials. We would probably find a rational explanation for that if we consistently included the Louie-Froyen-Cohen nonlinear core corrections in all of our pseudoions. We did not do that because this density-dependent correction does not lend

TABLE VII. Bulk properties of Na crystal (see text). The differences between frozen- and relaxed-core results are negligible. Experimental data are from Ref. [64].

	Lattice constant (\AA)	Cohesive energy (eV/atom)	Bulk modulus (kbar)
PH	4.19	0.86	75
Nonlocal	3.87	1.15	110
Full core	4.08	1.21	94
Expt.	4.20	1.13	68

itself to an extension to quantum Monte Carlo valence-only simulations [54], which were the motivation for local pseudo-Hamiltonians in the first place.

Our guess is that, at the subtle level of the silicon discrepancies just mentioned, but even to explain some of the sodium results (Tables VI and VII), one would probably discover that the pseudo-Hamiltonian tends to compensate exchange-correlation and Hartree errors, in the sense discussed by Teter [17], in a slightly more efficient way than standard nonlocal pseudopotentials. Systematic hardness tests as well as a complete tabulation of pseudo-Hamiltonians for the *sp* elements represent the natural extension of this work, and are under way [32].

ACKNOWLEDGMENTS

We thank D. M. Ceperley and M. Foulkes for useful discussions. Special thanks are due to L. Mitáš who taught us what a RST is and for many discussions about stochastic methods. Thanks are also due to A. Continenza for providing us with the results of an independent FLAPW calculation for the silicon crystal. Stefano Baroni and Michael Methfessel made their PPPW and FPLMTO codes available for crystal calculations. This work was partially supported by the Italian National Research Council (CNR) through “Progetto Finalizzato Sistemi Informatici e Calcolo Parallelo” under Grants No. 89.0006.69 and No. 89.00051.69.

APPENDIX: INTEGRATION OF THE KOHN-SHAM EQUATIONS

We sketch briefly how we solve numerically the radial Kohn-Sham Eqs. (22). The need to recall a number of known things is related to a few key choices in the construction of the cost function (see text). The Kohn-Sham equations involve the unknown eigenvalues ϵ_ℓ and eigenvectors $\chi_\ell(r)$ and the density

$$n(r) = \frac{1}{4\pi r^2} \sum_\ell f_\ell |\chi_\ell(r)|^2, \quad (\text{A1})$$

where f_ℓ is the occupation of the Kohn-Sham orbital $\chi_\ell(r)$. The density is responsible for the screening potential $v_{HXC}(r)$ through Eq. (19) and the self-consistent solution is found by standard iteration schemes. The way we solve each of the Eqs. (22) for a given trial density,

that is, a given potential $v_{HXC}(r)$, is the following. Once we have fixed the value of the angular momentum ℓ , for each value of the energy $\epsilon < 0$ the Kohn-Sham equations admit a solution $\chi_\ell^{IN}(\epsilon, r)$ and a solution $\chi_\ell^{OUT}(\epsilon, r)$, such that [67,34]

$$\chi_\ell^{IN}(\epsilon, r) \stackrel{r \rightarrow 0}{\approx} c_1 r^{\ell+1} + O(r^{\ell+3}), \quad (\text{A2})$$

$$\chi_\ell^{OUT}(\epsilon, r) \stackrel{r \rightarrow +\infty}{\approx} c_2 \exp(-\sqrt{-2\epsilon}r), \quad (\text{A3})$$

and they can be easily calculated for any negative energy ϵ on a finite numerical grid (following, e.g., Hamann [24]). If, after rescaling one of the two to match the other one at a radius R [68]

$$\chi_\ell^{IN}(\epsilon, R) = \chi_\ell^{OUT}(\epsilon, R), \quad (\text{A4})$$

we find that also the first derivatives happen to exactly match in R

$$\chi_\ell'^{IN}(\epsilon, R) = \chi_\ell'^{OUT}(\epsilon, R), \quad (\text{A5})$$

then we have found the eigenvalue $\epsilon_\ell = \epsilon$ and the corresponding eigenfunction. The difference $\chi_\ell^{IN}(\epsilon, R) - \chi_\ell^{OUT}(\epsilon, R)$ is then a measure of the departure of ϵ from the eigenvalue ϵ_ℓ [69] and, to first order in this energy difference, the eigenvalue can be estimated from

$$\epsilon_\ell \simeq \epsilon + \frac{1}{2} [\chi_\ell'^{IN}(\epsilon, R) - \chi_\ell'^{OUT}(\epsilon, R)] \chi_\ell^{OUT}(\epsilon, R). \quad (\text{A6})$$

As known, the above formula yields the eigenvalue ϵ_ℓ within the machine precision in a few iterations. The reason why we recall this known procedure here is to point out that we do not even need those iterations in our present scheme. During our simulated-annealing run we take $R = r_c$ and, for each new trial pseudo-Hamiltonian, we only need to integrate once $\chi_\ell^{IN}(\epsilon, r)$ at the full-core eigenenergy $\epsilon = \epsilon_\ell^{FC}$. Our final pseudo-Hamiltonian must satisfy Eqs. (37) and (38): the wave function χ_ℓ and its radial derivative χ_ℓ' must simply be identical to the full-core counterparts beyond R , and thus Eq. (A6) enables us to estimate the distance between the full-core target eigenvalue ϵ_ℓ^{FC} and the eigenvalue of the current trial pseudo-Hamiltonian. This clarifies the equivalence of $d[x_\ell(\epsilon_\ell^{FC}, r_c), x_\ell^{FC}(\epsilon_\ell^{FC}, r_c)]$ and $d(\epsilon_\ell, \epsilon_\ell^{FC})$, which was stated in Sec. III B, and the convenience of using $d[x_\ell(\epsilon_\ell^{FC}, r_c), x_\ell^{FC}(\epsilon_\ell^{FC}, r_c)]$, which requires just one integration, instead of using $d(\epsilon_\ell, \epsilon_\ell^{FC})$, which requires many iterative integrations.

-
- [1] *Monte Carlo Method in Statistical Physics*, edited by K. Binder (Springer-Verlag, Berlin, 1979); *Applications of the Monte Carlo Method in Statistical Physics*, 2nd ed., edited by K. Binder (Springer-Verlag, Berlin, 1987).
 - [2] D. M. Ceperley, *J. Stat. Phys.* **43**, 815 (1986).
 - [3] B. L. Hammond, P. J. Reynolds, and W. A. Lester, Jr., *Phys. Rev. Lett.* **61**, 2312 (1988).
 - [4] S. Fahy, X. W. Wang, and S. G. Louie, *Phys. Rev. B* **42**, 3503 (1990).
 - [5] L. Mitáš, E. L. Shirley, and D. M. Ceperley, *J. Chem. Phys.* **95**, 3467 (1991); L. Mitáš (unpublished); L. Mitáš,

- R. M. Martin, and D. M. Ceperley (unpublished). The latter two papers deal with iron and nitrogen, respectively.
- [6] M. L. Cohen and V. Heine, in *Solid State Physics: Advances in Research and Applications*, edited by H. Ehrenreich, F. Seitz, and D. Turnbull (Academic, New York, 1970), Vol. 24, pp. 37–248.
- [7] W. E. Pickett, *Comput. Phys. Rep.* **9**, 115 (1989).
- [8] J. F. Annett, *Phys. Rev. Lett.* **69**, 2244 (1992).
- [9] D. R. Hamann, M. Schlüter, and C. Chiang, *Phys. Rev. Lett.* **43**, 1494 (1979).

- [10] G. B. Bachelet, D. M. Ceperley, and M. G. B. Chiochetti, *Phys. Rev. Lett.* **62**, 2088 (1989); M. Chiochetti, Master thesis, University of Trento, 1988.
- [11] W. M. C. Foulkes and M. Schlüter, *Phys. Rev. B* **42**, 11 505 (1990).
- [12] Transition metals could be recovered if the next inner s and p shells were included in the valence space, along with the valence s and d [T. Starkloff and J. D. Joannopoulos, *Phys. Rev. B* **16**, 5212 (1977)]. This strategy, however, adds eight new tightly bound valence electrons to each atom which make both traditional plane-wave and quantum Monte Carlo calculations impractical: only single-particle calculations based on local orbitals can benefit from such a prescription.
- [13] X. P. Li, D. M. Ceperley, and R. M. Martin, *Phys. Rev. B* **44**, 10 929 (1991).
- [14] R. M. Dreizler and E. K. U. Gross, *Density Functional Theory* (Springer-Verlag, Berlin, 1990); P. Hohenberg and W. Kohn, *Phys. Rev.* **136**, B864 (1964); W. Kohn and L. J. Sham, *Phys. Rev.* **140**, A1133 (1965).
- [15] P. H. Acioli and D. M. Ceperley (unpublished).
- [16] P. Focher, A. Lastri, M. Covi, and G. B. Bachelet, *Phys. Rev. B* **44**, 8486 (1991).
- [17] M. Teter, *Phys. Rev. B* **48**, 5031 (1993).
- [18] L. Serra, G. B. Bachelet, N. Van Giai, and E. Lipparini, *Phys. Rev. B* **48**, 14 708 (1993).
- [19] P. J. Reynolds, D. M. Ceperley, B. J. Alder, and W. A. Lester, Jr., *J. Chem. Phys.* **77**, 5593 (1982).
- [20] G. B. Bachelet, D. M. Ceperley, M. G. B. Chiochetti, and L. Mitáš, in *Progress in Electron Properties of Solids*, edited by E. Doni, R. Girlanda, G. Pastori Parravicini, and A. Quattropani (Kluwer, Dordrecht, 1989), p. 11.
- [21] N. F. Mott and H. S. W. Massey, *The Theory of Atomic Collisions* (Oxford, New York, 1965), p. 181.
- [22] If A and B were independent on r , one could prove that $G(\mathbf{r}, \mathbf{r}', \tau)$ would be positive at any $\tau > 0$ [23]. For A and B dependent on r , see L. Mitáš, Ph.D. thesis, University of Bratislava, 1990 and A. Bosin, Ph.D. thesis, University of Cagliari, 1995.
- [23] M. Reed and B. Simon, *Methods of Modern Mathematical Physics* (Academic, New York, 1978), Vol. 4, pp. 212–213.
- [24] D. R. Hamann, *Phys. Rev. B* **40**, 2980 (1989).
- [25] D. M. Ceperley and B. J. Alder, *Phys. Rev. Lett.* **45**, 566 (1980).
- [26] J. Perdew and A. Zunger, *Phys. Rev. B* **23**, 5048 (1981).
- [27] Only f metals and a few other neighboring heavy elements would suffer from the lack of an accurate f wave, but for these elements both the DFT-LDA and the pseudopotential approximation are highly questionable anyway.
- [28] G. P. Kerker, *J. Phys. C* **13**, L189 (1980).
- [29] E. L. Shirley, D. C. Allan, R. M. Martin, and J. D. Joannopoulos, *Phys. Rev. B* **40**, 3652 (1989).
- [30] A. Lastri, Master thesis, University of Trento, 1991.
- [31] When for a given pseudoion two different operators—the ordinary nonlocal pseudopotential and the pseudo-Hamiltonian we describe in this paper—have a common, identical reference state (the same occupied single-particle orbitals, the same single-particle eigenvalues, the same electronic density, and thus the same value for the Kohn-Sham energy functional) the limits and virtues of those transferability criteria which are all based on various differential properties of the pseudoion taken at some reference state (e.g., the norm conservation or the “chemical hardness” recently proposed by Teter [17]) become more evident. The norm inside the core is identical and thus the two ions behave identically to first order in energy, but, precisely because the single-particle orbitals are the same, the higher order energy derivatives of the logarithmic derivative of their single-particle orbitals will more or less disagree, as discussed here; Teter’s chemical hardness is identical if the valence orbitals are identical at the reference state, but the two ions will not, in fact, be equally transferable because of the self-consistency terms which were neglected in his definition, as discussed elsewhere [32]. It seems fair to conclude that, since the “ultimate” transferability test (the actual comparison of full-core and pseudopotential calculations for molecular and solid-state systems) is seldom handy and conceptually not very satisfactory, a good criterion for ionic transferability is obtained by monitoring both logarithmic derivatives and chemical hardness at two or three (chemically meaningful) different reference states.
- [32] A. Filippetti, A. Bosin, and G. B. Bachelet (unpublished).
- [33] G. B. Bachelet, D. R. Hamann, and M. Schlüter, *Phys. Rev. B* **26**, 4199 (1982).
- [34] A. Bosin, Master thesis, University of Trento, 1990.
- [35] V. I. Smirnov, *A Course of Higher Mathematics* (Pergamon, Oxford, 1964), Vol. 3, Part 2, p. 367.
- [36] Especially in view of the subsequent use of the pseudo-Hamiltonian.
- [37] Of course, adding more and more constraints may result in increasing difficulties and ultimately make it impossible to build the desired pseudo-Hamiltonian.
- [38] As we will discuss in Sec. IV C, this additional constraint does sometimes (although not always, see Refs. [17,29]) improve the transferability of pseudoions.
- [39] W. H. Press, B. P. Flannery, S. A. Teukolsky, and W. T. Vetterling, *Numerical Recipes* (Cambridge University Press, New York, 1986).
- [40] N. Metropolis, A. W. Rosenbluth, M. N. Rosenbluth, A. H. Teller, and E. Teller, *J. Chem. Phys.* **21**, 1087 (1953).
- [41] S. Kirkpatrick, C. D. Gelatt, and M. P. Vecchi, *Science* **220**, 671 (1983).
- [42] P. J. M. van Laarhoven and E. H. L. Aarts, *Simulated Annealing: Theory and Applications* (Reidel, Dordrecht, 1987).
- [43] D. Vanderbilt and S. G. Louie, *J. Comput. Phys.* **56**, 259 (1984).
- [44] A. Bosin, CNR Technical Report No. 1/157, 1993 (unpublished).
- [45] L. Mitáš and G. B. Bachelet (unpublished).
- [46] In practice the best strategy to gradually “freeze” the system into its global minimum is to start the random walk with a relatively high temperature and then to reduce it as the random walk proceeds.
- [47] L. Mitáš and H. Mitášová, *Comput. Math. Applic.* **16**, 983 (1988).
- [48] A. Talmi and G. Gilat, *J. Comput. Phys.* **23**, 93 (1977).
- [49] A. Bosin, V. Fiorentini, A. Lastri, and G. B. Bachelet, in *Materials Theory and Modeling*, edited by P. D. Bristowe, J. Broughton, and J. M. Newsam, MRS Symposia Proceedings No. 291 (Materials Research Society, Pittsburgh, 1993), p. 21.
- [50] This Bachelet-Ceperley-Chiochetti-like pseudo-Hamil-

- tonian [10] is generated from a nonlocal pseudopotential which differs from the Bachelet-Hamann-Schlüter carbon [33] only by a 30% larger core radius. The parameters used to build the pseudo-Hamiltonian are $r_c = 1.2$, $k = 5$, and $a_0 = -0.95$.
- [51] S. G. Louie, S. Froyen, and M. L. Cohen, Phys. Rev. B **26**, 1738 (1982).
- [52] U. von Barth and C. D. Gelatt, Phys. Rev. B **21**, 2222 (1980).
- [53] The difference for $R^{-1} \rightarrow 0$ is due to the choice of the reference state: the ground state is the reference state for the nonlocal pseudopotentials but not for the pseudo-Hamiltonian (Sec. IV B). Hence, while nonlocal pseudopotentials and full-core atoms have the same eigenvalues for $R^{-1} \rightarrow 0$ (ground state), pseudo-Hamiltonian eigenvalues are shifted even for $R^{-1} \rightarrow 0$.
- [54] G. Galli, D. M. Ceperley, and G. B. Bachelet (unpublished).
- [55] M. Methfessel, Phys. Rev. B **38**, 1537 (1988).
- [56] V. Fiorentini, M. Methfessel, and M. Scheffler, Phys. Rev. B **47**, 13 353 (1993).
- [57] O. K. Andersen, O. Jepsen, and D. Glötzel, in *Highlights of Condensed Matter Theory*, edited by F. Bassani, F. Fumi, and M. P. Tosi (North-Holland, Amsterdam, 1985).
- [58] H. J. Monkhorst and J. D. Pack, Phys. Rev. B **13**, 5188 (1976).
- [59] M. J. Gillan, J. Phys. Condens. Matter **1**, 689 (1989).
- [60] A. De Vita (private communication).
- [61] M. Methfessel and A. T. Paxton, Phys. Rev. B **40**, 3616 (1989).
- [62] R. J. Needs, R. M. Martin, and O. H. Nielsen, Phys. Rev. B **33**, 3778 (1986).
- [63] C.-L. Fu and K.-M. Ho, Phys. Rev. B **28**, 5480 (1983).
- [64] *Physics of Group IV Elements and III-V Compounds*, edited by K. H. Hellwege and O. Madelung, Landolt-Börnstein New Series, Group III, Vol. 17, Pt. a (Springer, New York, 1987); *Intrinsic Properties of Group IV Elements and III-V, II-IV, and I-VII Compounds*, edited by K. H. Hellwege and O. Madelung, Landolt-Börnstein New Series, Group III, Vol. 22, Pt. a (Springer, New York, 1987).
- [65] C. Filippi and C. J. Umrigar (unpublished).
- [66] A. Continenza (private communication).
- [67] See, for example, L. D. Landau and E. M. Lifschitz, *Quantum Mechanics: non-relativistic theory* (Pergamon, London, 1958).
- [68] A convenient value for R is the so-called classical turning point, defined by $v(r) \geq \epsilon_l \forall r \geq R$. With this choice R is the radius where the radial wave function starts to decay to zero after having reached its outermost maximum, because the region outside R corresponds to a classically forbidden region. So if R is chosen, as we do, as the classical turning point, then we always have $R > r_c$: our core radius r_c is always between the outermost node and the outermost maximum of the relevant valence wave function, while R is always beyond the outermost maximum.
- [69] To distinguish between the different states of the same angular momentum, we count the number of (radial) nodes of $\chi_l^{IN}(\epsilon, r)$. For the lowest energy state such a number must be 0. If it is not, the energy ϵ is too high and must be diminished.